Int. J. Cancer: 108, 464–472 (2004)

Publication of the International Union Against Cancer

SYNERGISTIC INTERACTION BETWEEN THE EGFR TYROSINE KINASE INHIBITOR GEFITINIB ("IRESSA") AND THE DNA TOPOISOMERASE I INHIBITOR CPT-11 (IRINOTECAN) IN HUMAN COLORECTAL CANCER CELLS

Fumiaki KOIZUMI[1], Fumihiko KANZAWA[3], Yutaka UEDA[1], Yasuhiro KOH[3], Shoji TSUKIYAMA[3], Fumiko TAGUCHI[1,3], Tomohide TAMURA[2], Nagahiro SAIJO[2] and Kazuto NISHIO[1,3]*

[1]*Support Facility of Project Ward, National Cancer Center Hospital, Tokyo, Japan*
[2]*Medical Oncology, National Cancer Center Hospital, Tokyo, Japan*
[3]*Pharmacology Division, National Cancer Center Research Institute, Tokyo, Japan*

Epidermal growth factor receptor [EGFR (HER1, erbB1)] is a receptor with associated tyrosine kinase activity, and is expressed in colorectal cancers and many other solid tumors. We examined the effect of the selective EGFR tyrosine kinase inhibitor (EGFR-TKI) gefitinib ("Iressa") in combination with the DNA topoisomerase I inhibitor CPT-11 (irinotecan) on human colorectal cancer cells. EGFR mRNA and protein expression were detected by RT-PCR and immunoblotting in all 7 colorectal cancer cell lines studied. Gefitinib inhibited the cell growth of the cancer cell lines *in vitro* with an IC_{50} range of 1.2–160 μM by 3,(4,5-dimethyl-2-thiazolyl)-2,5-diphenyl-2H-tetrazolium bromide (MTT) assay. Lovo cells exhibited the highest level of protein and autophosphorylation of EGFR and were the most sensitive to gefitinib. The combination of gefitinib and CPT-11 induced supra-additive inhibitory effects in COLO320DM, WiDR and Lovo cells, assessed by an *in vitro* MTT assay. Administration of gefitinib and CPT-11 had a supra-additive inhibitory effect on WiDR cells and tumor shrinkage was observed in Lovo cell xenografts established in nude mice, whereas no additive effect of combination therapy was observed in COLO320DM cells. To elucidate the mechanisms of synergistic effects, the effect of CPT-11-exposure on phosphorylation of EGFR was examined by immunoprecipitation. CPT-11 increased phosphorylation of EGFR in Lovo and WiDR cells in time- and dose-dependent manners. This EGFR activation was completely inhibited by 5 μM gefitinib and gefitinib-induced apoptosis was enhanced by combination with CPT-11, measured by PARP activation although no PARP activation was induced by 5 μM CPT-11 alone. These results suggested that these modification of EGFR by CPT-11, in Lovo cells, is a possible mechanism for the synergistic effect of CPT-11 and gefitinib. These findings imply that the EGFR-TKI gefitinib and CPT-11 will be effective against colorectal tumor cells that express high levels of EGFR, and support clinical evaluation of gefitinib in combination with CPT-11, in the treatment of colorectal cancers.
© *2003 Wiley-Liss, Inc.*

Key words: *combination; gefitinib; "Iressa"; colorectal cancer; irinotecan*

Colorectal cancer is a major public health concern. Although chemotherapy appears to be of very limited value in advanced colorectal cancer, there have been many efforts to apply combination chemotherapy in patients with primary disease.[1–3]

The combination of fluorouracil and leucovorin used to be recognized as standard therapy for colorectal cancer, but the topoisomerase I inhibitor, irinotecan (CPT-11), has recently been demonstrated to be active against colorectal cancer that was resistant to prior therapy.[4,5] Moreover, the CPT-11/5-FU/LV combination has been approved as standard chemotherapy by the US FDA for metastatic colorectal cancer.[6] However, patients treated with CPT-11 plus bolus 5-FU/leucovorin have been found to have a 3-fold higher rate of treatment-induced or treatment-exacerbated death than patients treated with other arms of the respective studies.[7] We have therefore been seeking a new combination regimen containing CPT-11 and target-based drugs.

The development of target-based drugs, including receptor tyrosine kinase inhibitors (TKI), is one of the promising strategies for cancer chemotherapy.[8,9] Colorectal cancers express receptors of the type 1 tyrosine kinase family, including epidermal growth factor receptor (EGFR) and c-erbB-2,[10–12] and the EGFR has emerged as a central molecular target for modulation in cancer therapeutics. The correlation between high expression of EGFR and clinically aggressive malignant disease has made EGFR a promising target of therapy for many epithelial tumors, which represent approximately 2/3 of all human cancers. In solid cancers, including colorectal cancers, high EGFR expression correlates with poor prognosis.[11] Gefitinib ("Iressa") is an orally active, selective EGFR-TKI that blocks signal transduction pathways involved in the proliferation and survival of cancer cells and in other host-dependent processes promoting cancer growth.[13,14] In EGFR tyrosine kinase assays, gefitinib has an IC_{50} of 0.033 μM. Inhibition of c-erbB-2 and KDR occurs at doses 100-fold higher than for EGFR inhibition.[15] We have previously demonstrated that gefitinib exerts high growth-inhibitory activity against EGFR-positive tumors in a xenograft model,[16] and gefitinib is therefore expected to be a potent therapeutic agent against EGFR-positive colorectal cancers. In recent years, it has been shown that the combined treatment of established human colorectal cancer xenograft with anti-EGFR drug (cetuximab or gefitinib) and with topoisomerase I inhibitor, topotecan, increase the antitumor activity of these drugs.[17,18] The aim of the present study was to investigate the combination effect of gefitinib and CPT-11 and to elucidate the biochemical mechanism of synergistic interaction in colorectal cancers.

MATERIAL AND METHODS

Drugs and chemicals

Gefitinib (N-(3-chloro-4-fluorophenyl)-7-methoxy-6-[3-(morpholin-4-yl)propoxy] quinazolin-4-amine) was provided by AstraZeneca (Cheshire, UK). Gefitinib was dissolved in dimethyl sulfoxide (DMSO) for the *in vitro* study and suspended in 5% glucose, pH 6, for the *in vivo* study. CPT-11 was obtained from Yakult Honsha (Tokyo, Japan). CPT-11 was dissolved in 45 mg/ml solvitol (pH 3-4) for both the *in vivo* and *in vitro* studies.

*Correspondence to: Support Facility of Project Ward, National Cancer Center Hospital, 5-1-1 Tsukiji, Chuo-ku, Tokyo, 104-0045, Japan. Fax: +81-3-3547-5185. E-mail: knishio@gan2.res.ncc.go.jp

Received 19 May 2003; Revised 2 August 2002; Accepted 22 August 2003

DOI 10.1002/ijc.11539

Animals

Female BALB/c nude mice, 6-weeks-old, were purchased from Japan Charles River Co., Ltd. (Atsugi, Japan). All mice were maintained in our laboratory under specific-pathogen-free conditions.

Cells and culture

Human colorectal cancer cell lines WiDR, LS-174T, COLO320DM, COLO320HSR, Lovo, SW480 and HCT116 were obtained from ATCC (Lockville, MD). Lovo cells, SW480 and HCT116 cells were maintained in HAM's F12 medium (GIBCO BRL, Grand Island, NY), Leibovitz's L-15 medium and McCoy's 5A medium (GIBCO BRL), respectively, all supplemented with 10% heat-inactivated fetal bovine serum (FBS). Other cell lines were maintained in RPMI1640 (Nikken Bio Med. Lab., Kyoto, Japan) supplemented with 10% FBS.

Growth-inhibition assay

We used the tetrazolium dye [3,(4,5-dimethyl-2-thiazolyl)-2,5-diphenyl-2H-tetrazolium bromide, MTT] assay to evaluate the cytotoxicity of various drug concentrations. A 200 ml volume of an exponentially growing cell suspension (5×10^3–1.5×10^4 cells/ml) was seeded into a 96-well microtiter plate and 20 μl of each drug at various concentrations was added. After incubation for 72 hr at 37°C, 20 μl of MTT solution (5 mg/ml in phosphate buffered saline, PBS) was added to each well and the plates were incubated for a further 4 hr at 37°C. After centrifuging the plates at 200*g* for 5 min, the medium was aspirated from each well, and 180 μl of DMSO was added to each well to dissolve the formazan. Optical density was measured at 562 and 630 nm with a Delta Soft ELISA analysis program interfaced with a Bio-Tek Microplate Reader (EL-340, Bio-Metallics, Princeton, NJ). Each experiment was performed in 6 replicate wells for each drug concentration and carried out independently 3 or 4 times. The IC_{50} value was defined as the concentration needed for a 50% reduction in the absorbance calculated based on the survival curves. Percent survival was calculated as follows: (mean absorbance of 6 replicate wells containing drugs − mean absorbance of 6 replicate background wells)/(mean absorbance of 6 replicate drug-free wells − mean absorbance of 6 replicate background wells) × 100.

RT-PCR

Specific primers designed for EGFR CDS were used for detection of EGFR mRNA as described elsewhere.[16] First-strand cDNA was synthesized from the cells' RNA with an RNA PCR Kit (TaKaRa Biomedicals, Ohtsu, Japan). After reverse transcription of 1 μg of total RNA with Oligo(dT)-M4 adaptor primer, the whole mixture was used for PCR with 2 oligonucleotide primers (5′-AATGTGAGCAGAGGCAGGGA-3′,5′GGCTTGGTTTG-GAGCTTCTC-3′). PCR was performed with initial denaturation at 94°C for 2 min, 25 cycles of amplification (denaturation at 94°C for 30 sec, annealing at 55°C for 60 sec and extension at 72°C for 105 sec).

Immunoprecipitation and immunoblotting

The cultured cells were washed twice with ice-cold PBS, lysed in EBC buffer (50 mM Tris-HCl, pH 8.0, 120 mM NaCl, 0.5% Nonidet P-40, 100 mM NaF, 200 mM Na orthovanadate and 10 mg/ml each of leupeptin, aprotinin and phenylmethylsulfonyl fluoride). The lysate was cleared by centrifugation at 20,000*g* for 5 min, and the protein concentration of the supernatant was measured by BCA protein assay (Pierce, Rockford, IL). For Immunoblotting, 20 μg samples of protein were electrophoretically separated on a 7.5% SDS-polyacrylamide gel and transferred to a polyvinylidene difluoride (PVDF) membrane (Millipore, Bedford, MA). The membrane was probed with rabbit polyclonal antibody against EGFR (1005; Santa Cruz Biotech, Santa Cruz, CA), HER2/neu (c-18; Santa Cruz), phospho-EGFR specific for Tyr 845, Tyr 1045, and Tyr 1068 (numbers 2231, 2235 and 2234; Cell Signaling, Beverly, MA) and cleaved PARP (number 9544; Cell Signaling) as the first antibody, followed by horseradish peroxidase-conjugated secondary antibody. The bands were visualized by electrochemiluminescence (ECL, Amersham, Piscataway, NJ). For immunoprecipitation, 5×10^6 cells were washed, lysed in EBC buffer, and centrifuged. The resultant supernatants (1,500 μg) were incubated with the anti-EGFR antibody (1005) at 4°C overnight. The immunocomplex were absorbed onto protein A/G-Sepharose beads, washed 5 times with lysate buffer, denatured and subjected to electrophoresis on a 7.5% polyacrylamide gel followed by immunostaining probed with antiphosphotyrosine antibody (PY-20, BD Bioscience Clontech, Tokyo, Japan).

Combined effect of gefitinib and CPT-11 in vitro

The combined effect of gefitinib and CPT-11 on colorectal cancer cell growth was evaluated by the combination index (CI) analysis method.[6] For any given drug combination, CI represents the degree of synergy, additivity or antagonism. CI was expressed in terms of fraction-affected (F_a) values, which represents the percentage of cells killed or inhibited by the drug. Using the mutually exclusive ($\alpha=0$) or mutually nonexclusive ($\alpha=1$) isobologram equation, the F_a/CI plots for each cell line was constructed by computer analysis of the data generated from the median effect analysis. CI values were interpreted as follows: <1.0 = synergism; 1.0 = additive and >1.0 = antagonism.

Using the median-effect method, developed by Chou and Talalay, the dose-response curve was plotted for each drug and for multiple doses of a fixed-ratio combination by using the equation:

$$f_a/f_u = (D/D_m)^m,$$

where, D is the dose-administered, Dm is the dose required for 50% inhibition of growth, f_a is the fraction affected by dose D, f_u is the unaffected fraction and m is a coefffect curve. The dose-response curve was plotted by logarithmic conversion of the equation to determine the m and D_m values, and the dose D_x required for x percent effect $(f_a)_x$ was then calculated as

$$D_x = D_m[f_a]_x/(f_u)x]^{1/m}.$$

Thus, CI can be defined by the isobologram equation

$$CI = (D)_1/(D_x)^1 + (D)_2/(D_x)2 + \alpha(D)_1(D)_2/(D_x)_1(D_x)_2,$$

where $(D_x)_1$ is the dose of Drug-1 required to produce x percent effect alone, and $(D)_1$ is the dose of Drug 1 required to produce the same x percent effect in combination with Drug 2; similarly, $(Dx)_2$ is the dose of Drug 2 required to produce x percent effect alone and $(D)_2$ is the dose of Drug 2 required to produce the same x percent effect in combination with Drug 1. Theoretically, CI is the ratio of the combined dose to the sum of the single-drug doses at an isoeffective level. Consequently, CI values <1 indicate synergism, values >1 indicate antagonism and a value of 1 indicates additive effects. The CI values obtained from both the classical nonconservative ($\alpha=0$) and conservative ($\alpha=1$) isobologram equations are presented in this report.

Growth-inhibition assay in vivo

Experiments were performed in accordance with the United Kingdom Coordinating Committee on Cancer Research Guidelines for the welfare of animals in experimental neoplasia (second edition).

In vivo experiments were scheduled to evaluate the combined therapeutic effect on preexisting tumors of oral or intraperitoneal administration of gefitinib and intravenous injection of CPT-11. The dose of each drug was set based on the results of a preliminary experiment involving administration of each drug alone. Ten days before administration, 1×10^7 WiDR and COLO320DM or 2×10^6 Lovo cells were injected subcutaneously into the back of mice. Five or 6 mice per group were injected with tumor cells. Tumor bearing mice were either given gefitinib, 40 mg/kg/day *p.o.* on days 1–10, or CPT-11, 40 mg/kg/day *i.v.* on days 1, 5 and 9, or

both, or placebo (5%(w/v) glucose solution). Alternatively, gefitinib, 30 or 60 mg/kg, *i.p.* days 1–14, and *i.v.* CPT-11, 16.7 or 33.3 mg/kg, *i.v.* on days 1, 5 and 9, were administered to the mice. Tumor diameters were measured with calipers on days 1, 4, 7, 10, 14, 18 and 22 to evaluate the effects of treatment, and tumor volume was determined by using the following equation: tumor volume = $ab^2/2$ (mm^3) (where a is the largest diameter of the tumor and b is the shortest diameter). Day "x" denotes the day on which the effect of the drugs was estimated, and day "0" denotes the first day of treatment. All mice were sacrificed on day 22 after measuring their tumors.

Statistical analysis

Differences between the test groups were analyzed by 1-factor ANOVA followed by Fisher's protected least significant difference (PLSD). A value of $p<0.05$ was considered statistically significant.

RESULTS

EGFR and HER2 expression and EGFR autophsophorylation in colorectal cancer cells

We examined EGFR mRNA expression by RT-PCR analysis using 2 specific primers. Approximately 570 bp-long PCR products were amplified in all cell lines that exhibited expression of EGFR mRNA (Fig. 1*a*). Comparison of the protein expression levels of EGFR in colorectal cancer cells by immunoblotting (Fig. 1*b*) revealed high expression in Lovo and WiDR cells. EGFR protein was also detected in LS-174T, COLO320DM, COLO320HSR, HCT116 and SW480 cells, although the expression levels in COLO320DM and COLO320HSR are subtle. The highest expression level of phosphrylated EGFR measured by phospho-specific EGFR antibody (Tyr845, Tyr1045 and Tyr1068) was observed in Lovo cells (Fig. 1*b*). Because the function of EGFR is closely related to that of other HER families including HER2/neu, we also examined the protein level of HER2/neu. High expression of HER2/neu were observed in LS-174T, HCT-116 and SW480 (Fig. 1*b*).

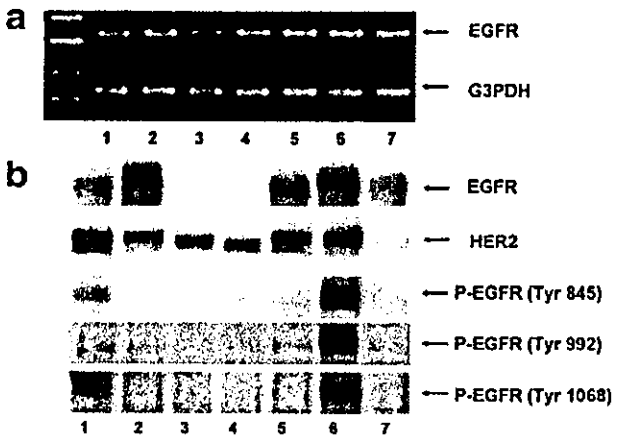

FIGURE 1 – EGFR expression in colorectal cancer cells. (*a*) Expression of EGFR mRNA in each cell line was detected by RT-PCR using specific primers designed for EGFR CDS. Expression of G3PDH mRNA was detected. Twenty-five cycles of PCR amplification were performed for each PCR product. Lanes 1–7 represent LS-174T, WiDR, COLO320DM, COLO320HSR, HCT116, Lovo and SW480 cells, respectively. (*b*) A 20 μg sample of total cell lysates was separated by 7.5% SDS-PAGE, transferred to PVDF membrane, and incubated with a specific anti-human EGFR, HER2/neu and phospho-EGFR (Tyr845, Tyr992 and Tyr1068).

Cellular sensitivity of colorectal cancer cells to gefitinib and CPT-11

The growth inhibitory effect of gefitinib and CPT-11 on colorectal cancer cells was examined by MTT assay. The IC_{50} values of gefitinib for the cell lines ranged from 1.2 μM (Lovo cells) to 160 μM (HCT116 cells) (Table I). No significant relationship was observed between EGFR expression levels and IC_{50} values among these cell lines. However, Lovo cells, which exhibited the highest EGFR expression and its phosphorylation, were the most sensitive to gefitinib. On the other hand, the IC_{50} values of CPT-11 for the cell lines ranged from 5.2 μM (Lovo) to 35 μM (SW480). The range of sensitivity to gefitinib was wider than to CPT-11.

In vitro *combined effect of gefitinib and CPT-11 on colorectal cancer cell lines*

Based on the results of the evaluation of *in vitro* growth-inhibition, 4 cell lines (WiDR, COLO320DM, Lovo, and SW480 cells) were selected for the *in vitro* combination study. Cells were treated with gefitinib or CPT-11 alone or in concomitant combination at fixed molar ratio for 72 hr. The ratios of gefitinib and CPT-11 were set based on the IC_{50} values of each cell line. Growth rate values are averages of data from at least 3 independent experiments. The effects of combinations of gefitinib and CPT-11 on cell growth are shown in Figure 2. CI values of <1, >1 and 1 indicate a supra-additive effect (synergism), antagonistic effect and additive effect, respectively. A low CI index was observed in WiDR, COLO320DM and Lovo cells over a wide range of inhibition levels. Synergistic effects were also observed in the relatively high F_a values in SW480 cells. These results suggest that gefitinib and CPT-11 had a synergistic effect on most of the colorectal cancer cell lines *in vitro*.

In vivo *combination effects of gefitinib and CPT-11*

In order to determine whether the combination of these 2 drugs is also synergistic against colorectal cancer *in vivo*, the growth-inhibitory effect of the combination was evaluated against the colorectal cancer cells in tumor xenografts. The growth inhibitory effect of gefitinib, 30 mg/kg, *i.p.* days 1–10, and CPT-11, 40 mg/kg, *i.v.* days 1, 5 and 9, on WiDR cells was evaluated (Fig. 3*a*,*b*). Administration of gefitinib or CPT-11 alone suppressed the tumor volume of WiDR cells with a T/C value of 73.9% and 69.2%, respectively, at day 22, (Fig. 3*c*), whereas gefitinib+CPT-11 suppressed WiDR tumors with T/C value of 51.8% at day 22, but this was not statistically significant (Fig. 3*d*, $p=0.164$ by 1-factor ANOVA). A 10% body weight loss was observed until day 15 in mice given the combination, but body weight recovered by day 22 (Fig. 3*e*). No growth inhibitory effect of single or combined therapy of CPT-11 and gefitinib in COLO320DM cells were observed (data not shown). In mice transplanted with Lovo cells, with a high EGFR expression level, marked tumor growth inhibition was achieved with gefitinib+CPT-11 (Fig. 3*f*). The T/C of the combination schedule at day 11 was 22.8% and significantly lower than in the control ($p<0.0012$ by Fisher's PSLD, Fig. 3*g*). A 10% maximum body weight loss until day 15 was also observed in mice treated with the combination (Fig. 3*j*).

Alternatively, the combined effect of oral administration of gefitinib and intravenous administration of CPT-11 was evaluated in mice transplanted with Lovo cells. Gefitinib, 30 or 60 mg/kg *p.o.* days 1–14, and CPT-11, 16.7 or 33.3 mg/kg *i.v.* days 1, 5 and 9, were administered (schedule 2, Fig. 4*a*), and greater growth inhibition was observed in mice treated with this combination, compared to the controls (Fig. 4*b*) A more marked growth-inhibitory effect was observed at a higher dose of CPT-11 (16.7 *vs.* 33.3 mg/kg), but there was no difference between 30 mg/kg and 60 mg/kg of gefitinib in the combination. The combination of gefitinib (30 and 60 mg/kg) and CPT-11 (33.3 mg/kg/*i.v.*) resulted in tumor reduction during treatment that was significant at day 15 (Fig. 4*c*). The T/C values imme-

TABLE I – *IN VITRO* GROWTH-INHIBITORY ACTIVITY OF GEFITINIB AND CPT-11 IN HUMAN COLORECTAL CANCER CELLS (MTT ASSAY)[1]

Cell line	gefitinib		CPT-11	
	IC_{50} (μM)	Concentration range (μM)	IC_{50} (μM)	Concentration range (μM)
WiDR	10 ± 1.1	0.83–53	33 ± 7.5	1.6–160
LS-174T	100.4 ± 10.1	N.D.	13	N.D.
COLO320DM	11 ± 3.8	0.63–100	11 ± 0.6	1.6–160
COLO320HSR	22	N.D.	5.5	N.D.
HCT116	177.0 ± 12.2	N.D.	11	N.D.
SW480	23 ± 0.6	1.6–10	35 ± 5.5	1.6–50
Lovo	1.2 ± 0.59	0.31–25	5.2 ± 0.82	0.16–10

[1]The IC_{50} value (μM) of each drug was measured by MTT assay, as described in the Materials and Methods. Each value is a mean ± SD of 3 or 4 independent experiments–N.D., not determined.

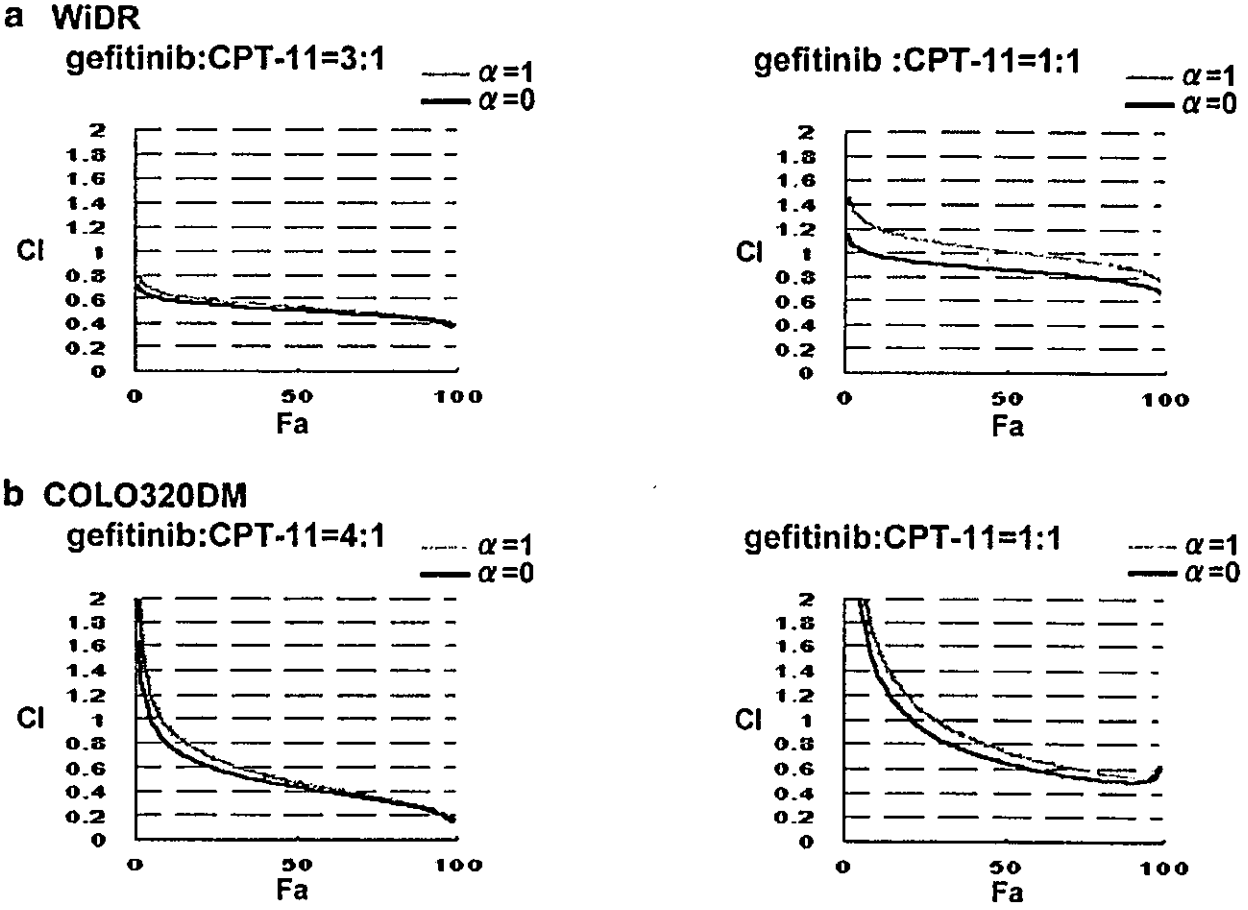

FIGURE 2 – Combination index (CI) plots of interactions between gefitinib and CPT-11. Cells were treated with gefitinib and CPT-11 alone and in combination at fixed molar ratios (molar ratios of gefitinib to CPT-11 of 3:1 and 1:1 [(*a*) WiDR], 4:1 and 1:1 [(*b*) COLO320DM], 1:2 and 1:5 [(*c*) Lovo], 1:1 [(d) SW480]. Using the mutually exclusive (CI) or mutually nonexclusive (CI') isobologram equation, the affected fraction (F_a)-CI plot for each cell was constructed by computer analysis of the data generated from the median effect analysis. CI values <1 occurred over a wide range of inhibition levels, indicating synergy.

diately after the completion of treatment (at day 15) and at day 22 are summarized in Fig.4*d*. More severe body weight loss was observed, ~20% at day 15, in mice treated with 60 mg/kg of gefitinib alone or with CPT-11, suggesting that CPT-11 does not enhance the body weight loss induced by gefitinib. Body weight recovered by day 22 (Fig. 4*e*). No deaths of were observed during the treatment or observation period.

Induction of EGFR phosphorylation and enhanced gefitinib-induced PARP activation by CPT-11

To elucidate the synergistic effects of CPT-11 and gefitinib, we examined the effect of exposure of CPT-11 on EGFR phosphorylation in Lovo and WiDr cells. Phosphorylated EGFR was detected with anti-phosphotyrosine antibody (PY-20)

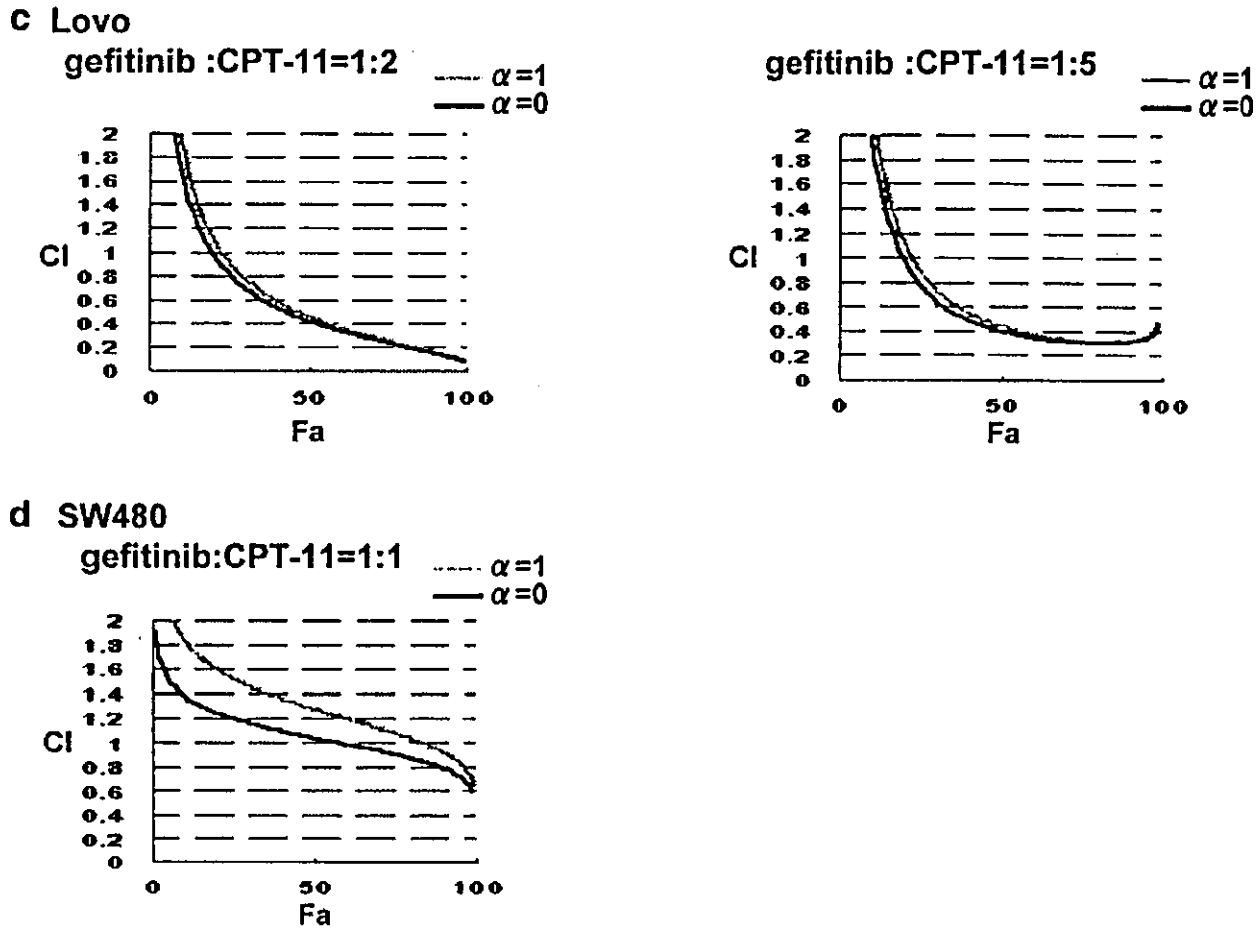

FIGURE 2 – CONTINUED.

against immunoprecipitated EGFR and increased phosphorylation of EGFR was observed after exposure to CPT-11 in Lovo cells in dose- and time- dependent manner (3–24 hr) (Fig. 5*a*). The dose-dependent activation of EGFR by CPT-11 was also obtained in WiDR cells (Fig. 5*b*). CPT-11-induced phosphorylation of EGFR was observed without ligand-stimulation. The EGFR activation was completely inhibited by 24 hd exposure of 5 μM gefitinib. gefitinib-induced apoptosis measured by PARP activation was enhanced by combination with CPT-11, although no PARP activation was induced by CPT-11 alone (Fig. 5*c*). These results suggest that the modification of EGFR by CPT-11 increases the cellular sensitivity to gefitinib, resulting the synergistic effect of CPT-11 and gefitinib. We also observed the effect of gefitinib on the expression and the activity of topoisomerase I by immunoblotting and decatenatnion assay. No modification of topoisomerase I by gefitinib was observed (data not shown).

DISCUSSION

Evidence has suggested that the new EGFR-targeting drug gefitinib is active against gastrointestinal malignancies as well as non-small cell lung cancer. Combination of gefitinib with cytotoxic drugs has been evaluated in the U.S. and Europe,[19,20] but combination with CPT-11 has not been evaluated. CPT-11 is a potent DNA-targeting drug in patients with colorectal cancer that is refractory to treatment with fluorouracil and leucovorin,[4,5] although a higher rate of treatment-induced toxicity was suspected in a retrospective analysis.[7] In preclinical study, Ciadiello *et al.*[17,18] reported that supra-additive combination effect of EGFR-targeting drug (cetuximab or gefitinib) and topoisomerase I inhibitor, topotecan was observed in human colorectal cancer GEO xenograft. We have therefore studied the synergistic potential for a new combination regimen containing CPT-11 and gefitinib. The synergistic potential of CPT-11 combined with gefitinib demonstrated in our study suggests that the gefitinib/CPT-11 combination is a promising regimen for colorectal cancer patients. Schedule 2, administration of oral gefitinib and intravenous CPT-11 designed in a xenograft model, was based on possible clinical administration of the drugs, and thus a treatment schedule consisting of intermittent *i.v.* CPT-11 and continuous gefitinib *p.o.* may be applicable to colorectal cancer in humans.

In xenograft models, body weight loss was observed when administered in combination as well as when each drug was administered alone. However, body weight loss rapidly recovered immediately after the completion of administration, and no deaths were observed. Diarrhea is the dose-limiting toxicity of CPT-11 in humans,[7] and it is also observed in patients treated with gefitinib.[21,22] However, no diarrhea or related phenomena were observed in the mouse model treated with combinations of these

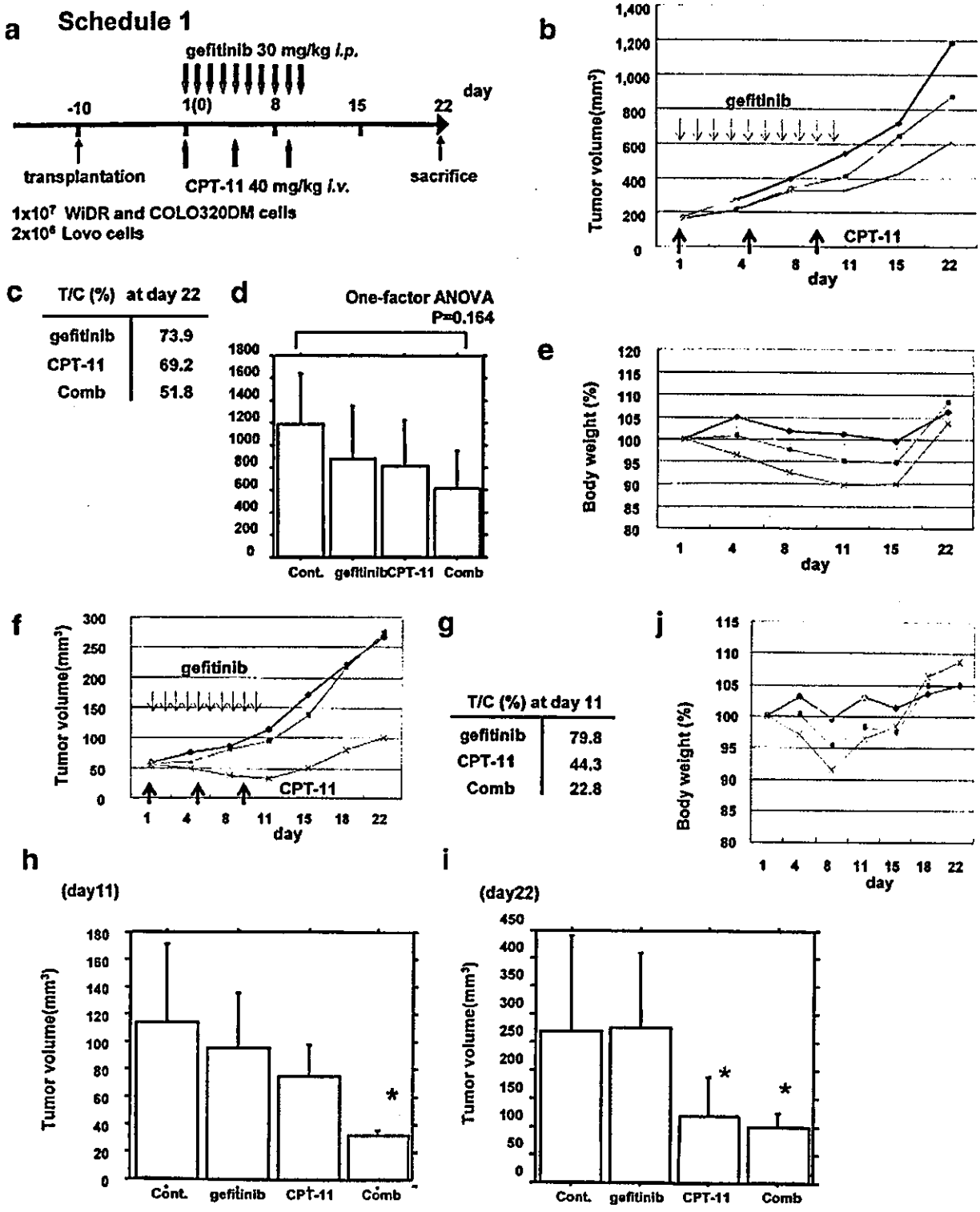

FIGURE 3 – *In vivo* combined effect of gefitinib and CPT-11 on WiDR and Lovo tumor xenografts. (*a*) Treatment schedule. (*b*) (WiDR) and F (Lovo), Tumor growth curves. Female nude mice bearing WiDR or Lovo xenografts were randomly allocated to treatment with 5% (w/v) glucose solution (diamond), gefitinib (square), CPT-11 (triangle), or the combination (×). Tumor volume was calculated as described in Material and Methods. Each data point represents the mean tumor volume of 5 mice. E (WiDR) and J (Lovo) Percent change in body weight in the gefitinib (hatched square) and combination (×) group. C (WiDR) and G (Lovo) Ratio of tumor volume in the control (C) to tumor volume in the treatment group (T) at day 22 and day 15. D (WiDR), H and I (Lovo) Histogram of mean tumor volume at day 11 and day 22 bars, *S.D.* Statistical analysis was performed by 1-factor ANOVA, followed by Fisher's PLSD between 2 groups, as described in the Material and Methods section. *Significant difference ($p<0.05$; Fisher's PLSD) compared to the control.

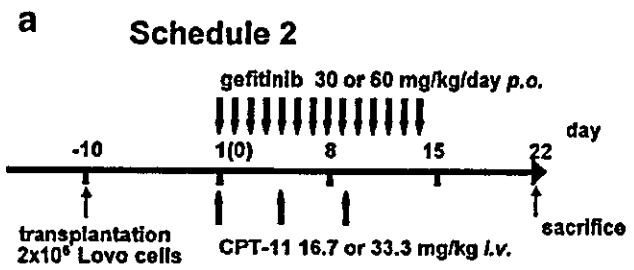

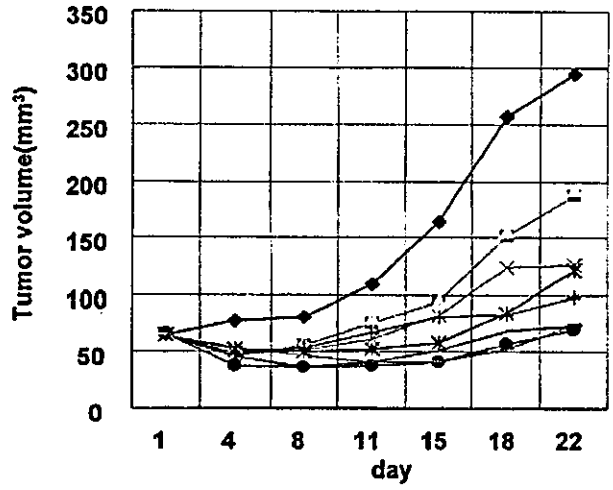

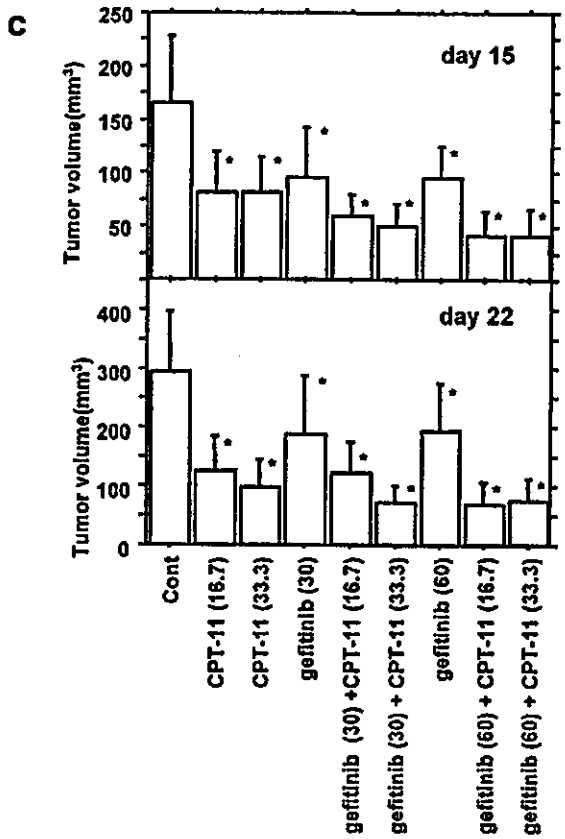

d

	T/C (%) at day 15
gefitinib 30	57.6
gefitinib 60	58.4
CPT-11 16.7	49.6
gefitinib 30+CPT-11 16.7	35.4
gefitinib 60+CPT-11 16.6	25.1
CPT-11 33.3	49.3
gefitinib 30+CPT-11 33.3	30.9
gefitinib 60+CPT-11 33.3	25.3

	T/C (%) at day 22
gefitinib 30	63.7
gefitinib 60	65.7
CPT-11 16.7	43.0
gefitinib 30+CPT-11 16.7	41.6
gefitinib 60+CPT-11 16.6	23.6
CPT-11 33.3	33.2
gefitinib 30+CPT-11 33.3	24.9
gefitinib 60+CPT-11 33.3	25.3

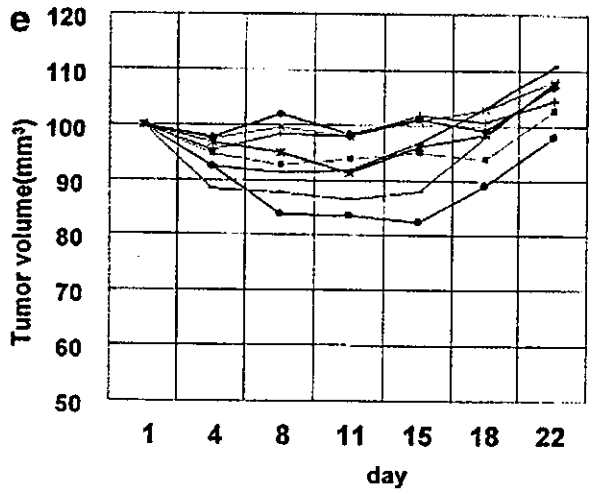

FIGURE 4 – The dose-dependent effect of combination therapy on Lovo cells *in vivo*. (*a*) Treatment schedule. (*b*) Significant growth-inhibition was observed in mice treated with the combination. Mice were allocated to 9 groups (6 mice/group) [closed diamond, 5%(W/V) glucose solution; ×, CPT-11 16.7 mg/kg; + CPT-11 33.3 mg/kg; square, gefitinib 30 mg/kg; star, gefitinib 30 mg/kg + CPT-11 16.7 mg/kg; blue line, gefitinib 30 mg/kg + CPT-11 33.3 mg/kg; open triangle, gefitinib 60 mg/kg; circle, gefitinib 60 mg/kg + CPT-11 16.7 mg/kg; light blue line, filled square, gefitinib 60 mg/kg + CPT-11 33.3 mg/kg]. (*c*) Mean tumor volumes and results of the statistical analysis at days 15 and 22, bars, *S.D.* *Significant difference ($p<0.05$) compared to the control. (*d*) T/C(%) at day 15 and 22. (*e*) Treatment-related body weight loss occurred in mice treated with gefitinib 60 mg/kg (triangle, circle, and light blue line).

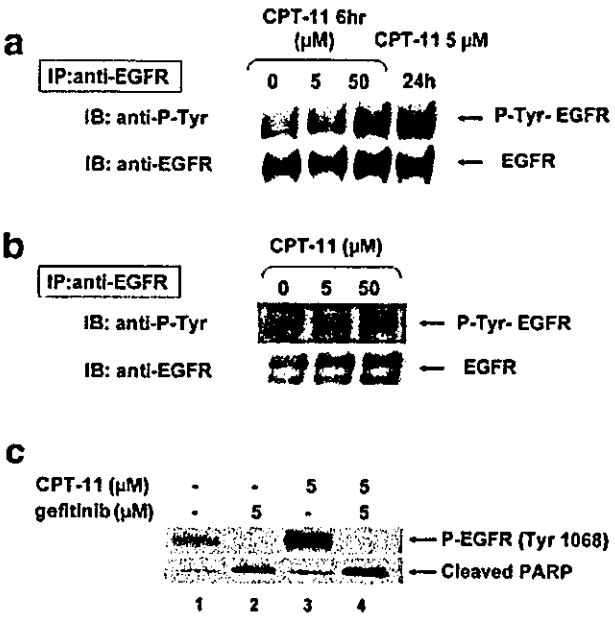

FIGURE 5 – The effect of CPT-11 on EGFR phosphorylation in WiDR cells. Lovo (*a*) and WiDR (*b*) cells (5×10^6) were treated with 5 or 50 μM CPT-11 for 6 hr. Additionally Lovo cells were treated with 5 μM CPT-11 for 24 hr. The 1,500 μg of total cell lysate was immunoprecipitated with an anti-EGFR antibody. Tyrosine-phosphorylated EGFR was determined with an anti-phosphotyrosine antibody and the membranes were reblotted by anti-EGFR antibody. (*c*) Lovo cells were treated with gefitinib or CPT-11 alone (lane 2 and 3) and in combination (lane 4) for 24 hr. A 20 μg of protein of each sample was analyzed by Western blotting using antiphospo-EGFR (Tyr 1068) and cleaved PARP antibody.

drugs. These results suggest that this regimen is intensive but can be tolerated, at least in mice.

The *in vitro* and *in vivo* experiments in our study demonstrated the synergistic potential of gefitinib – CPT-11 combination. We previously reported that topoisomerase I up-regulation by counter-part drugs was a possible mechanism for the synergy in an CPT-11 containing regimen.[23] On the other hand, the synergistic potential of gefitinib with topotecan, cisplatin, paclitaxel or radiation has been reported.[18,24–28] To elucidate the biochemical mechanism underlying the synergistic interaction between the gefitinib and CPT-11, the effect of CPT-11 on EGFR-phosphorylation was examined (Fig. 5). Increased phosphorylation of EGFR was observed after exposure to CPT-11 in dose and time-dependent manner in WiDR and Lovo cells. Since EGFR expression and phosphorylation were the major determining factors for sensitivity of the cells to gefitinib-induced growth-inhibition,[14] biochemical modulation of EGFR by CPT-11 might be responsible for the synergistic interaction between gefitinib and CPT-11. EGFR is induced and activated by cellular stress, such as oxidative stress and UV irradiation.[29–34] Ohmori *et al.*[22] demonstrated that increased autophosphorylation of EGFR was obtained in cisplatin-exposure in human lung cancer cells. A number of reports suggest that EGFR promotes cell survival through the activation of the ERK or the AKT pathway.[31,32] EGFR activation induced by these cellular stress may play a survival response against apoptosis.[31,32] In the present study, PARP activation by gefitinib was markedly enhanced by combination with CPT-11 at 5 μM exposure, which is comparable with IC_{50} value of CPT-11 in Lovo cells, although no PARP activation was observed by monotherapy of CPT-11. On the other hand, gefitinib does not modify the expression and the activation of topoisoerase I (data not shown). These result suggest that the inhibitory effect of gefitinib on the activated survival signal transduction induced by CPT-11 lead to synergistic effect. The findings of the present study suggest that biological modulation by various anticancer agents including DNA damaging agents will contribute to the synergistic effects of these anticancer agents and gefitinib in EGFR expressing tumor and support clinical evaluation of gefitinib in combination with DNA-targeting agents, especially CPT-11, in the treatment of colorectal cancers.

REFERENCES

1. Blijham G, Wagener T, Wils J, de Greve J, Buset M, Bleiberg H, Lacave A, Dalmark M, Selleslag J, Collette L, Sahmoud T. Modulation of high-dose infusional fluorouracil by low-dose methotrexate in patients with advanced or metastatic colorectal cancer: final results of a randomized European Organization for Research and Treatment of Cancer Study. J Clin Oncol 1996;14:2266–73.
2. O'Connell MJ, Klaassen DJ, Everson LK, Cullinan S, Wieand HS. Clinical studies of biochemical modulation of 5-fluorouracil by leucovorin in patients with advanced colorectal cancer by the North Central Cancer Treatment Group and Mayo Clinic. NCI Monogr 1987;185–8.
3. Focan C, Kreutz F, Focan-Henrard D, Moeneclaey N. Chronotherapy with 5-fluorouracil, folinic acid and carboplatin for metastatic colorectal cancer; an interesting therapeutic index in a phase II trial. Eur J Cancer 2000;36:341–7.
4. Shimada Y, Yoshino M, Wakui A, Nakao I, Futatsuki K, Sakata Y, Kambe M, Taguchi T, Ogawa N. Phase II study of CPT-11, a new camptothecin derivative, in metastatic colorectal cancer. CPT-11 Gastrointestinal Cancer Study Group. J Clin Oncol 1993;11:909–13.
5. Cunningham D, Pyrhonen S, James RD, Punt CJ, Hickish TF, Heikkila R, Johannesen TB, Starkhammar H, Topham CA, Awad L, Jacques C, Herait P. Randomised trial of irinotecan plus supportive care versus supportive care alone after fluorouracil failure for patients with metastatic colorectal cancer. Lancet 1998;352:1413–8.
6. Saltz LB, Cox JV, Blanke C, Rosen LS, Fehrenbacher L, Moore MJ, Maroun JA, Ackland SP, Locker PK, Pirotta N, Elfring GL, Miller LL. Irinotecan plus fluorouracil and leucovorin for metastatic colorectal cancer: Irinotecan Study Group. N Engl J Med 2000;343:905–14.
7. Rothenberg ML, Meropol NJ, Poplin EA, Van Cutsem E, Wadler S. Mortality associated with irinotecan plus bolus fluorouracil/leucovorin: summary findings of an independent panel. J Clin Oncol 2001;19:3801–7.
8. Modi S. Seidman AD. An update on epidermal growth factor receptor inhibitors. Curr Oncol Rep 2002;4:47–55.
9. Saijo N, Tamura T, Nishio K. Problems in the development of target-based drugs. Cancer Chemother Pharmacol 2000;46:S43–5.
10. Baselga J. The EGFR as a target for anticancer therapy: focus on cetuximab. Eur J Cancer 2001;37:S16–22.
11. Nicholson RI, Gee JM, Harper ME. EGFR and cancer prognosis. Eur J Cancer 2001;37:S9–15.
12. Speer G, Cseh K, Winkler G, Takacs I, Barna I, Nagy Z, Lakatos P. Oestrogen and vitamin D receptor (VDR) genotypes and the expression of ErbB-2 and EGF receptor in human rectal cancers. Eur J Cancer 2001;37:1463–8.
13. Albanell J, Rojo F, Baselga J. Pharmacodynamic studies with the epidermal growth factor receptor tyrosine kinase inhibitor ZD1839. Semin Oncol 2001;5:56–66.
14. Mendelsohn J, Baselga J. The EGF receptor family as targets for cancer therapy. Oncogene 2000;19:6550–65.
15. Woodburn JR, Morris CQ, Kelly H. EGF receptor tyrosine kinase inhibitors as anti-cancer agents-preclinical and early clinical profile of ZD1839. Cell Mol Biol Lett 1998;3:348–9.
16. Naruse I, Ohmori T, Ao Y, Fukumoto H, Kuroki T, Mori M, Saijo N, Nishio K. Antitumor activity of the selective epidermal growth factor receptor-tyrosine kinase inhibitor (EGFR-TKI) Iressa™ (ZD1839) in a EGFR-expressing multidrug resistant cell line in vitro and in vivo. Int J Cancer 2002;98:310–5.
17. Ciardiello F, Bianco R, Damiano V, De Lorenzo S, Pepe S, De Placido S, Fan Z, Mendelsohn J, Bianco AR, Tortora G. Antitumor activity of sequential treatment with topotecan and anti-epidermal

growth factor receptor monoclonal antibody C225. Clin Cancer Res 1999;5:909–16.
18. Ciardiello F, Caputo R, Bianco R, Damiano V, Pomatico G, De Placido S, Bianco A.R, Tortora G. Antitumor effect and potentiation of cytotoxic drugs activity in human cancer cells by ZD-1839 (Iressa), an epidermal growth factor receptor-selective tyrosine kinase inhibitor. Clin Cancer Res 2000;6:2053–63.
19. Sirotnak FM, Zakowski MF, Miller VA, Scher HI, Kris MG. Efficacy of cytotoxic agents against human tumor xenografts is markedly enhanced by coadministration of ZD1839 (Iressa), an inhibitor of EGFR tyrosine kinase. Clin Cancer Res 2000;6:4885–92.
20. Slichenmyer WJ, Fry DW. Anticancer therapy targeting the erbB family of receptor tyrosine kinases. Semin Oncol 2001;28:67–79.
21. Kusaba H, Tamura T, Nakagawa K, Yamamoto N, Kudoh S, Negoro S, Takeda K, Tanigawara Y, Fukuoka M. A phase I intermittent dose-escalation trial of ZD1839 ('IRESSA') in Japanese patients with solid malignant tumors. Clin Cancer Res 2000;6:abs381.
22. Kris M, Ranson M, Ferry D, Hammond L, Averbuch S, Ochs J, Rowinsky E. Phase I study of oral ZD1839('IRESSA'): A novel inhibitor of epidermal growth factor receptor tyrosine kinase (EGFR-TKI)—Evidence of good tolerability and activity. Clin Cancer Res 1999;5:abs 99
23. Kanzawa F, Koizumi F, Koh Y, Nakamura T, Tatsumi Y, Fukumoto H, Saijo N, Yoshioka T, Nishio K. In vitro synergistic interactions between the cisplatin analogue nedaplatin and the DNA topoisomerase I inhibitor irinotecan and the mechanism of this interaction. Clin Cancer Res 2001;7:202–9.
24. Ohmori T, Ao Y, Nishio K, Saijo N, Arteaga CL, Kuroki T. Low dose cisplatin can modulate the sensitivity of human non-small cell lung carcinoma cells to EGFR tyrosine kinase inhibitor (ZD1839; 'Iressa') in vivo. Proc Am Assoc Cancer Res 2000;41:abs 3072.
25. Magne N, Fischel JL, Dubreuil A, Formento P, Marcie S, Lagrange JL, Milano G. Sequence-dependent effects of ZD1839 ('Iressa') in combination with cytotoxic treatment in human head and neck cancer. Br J Cancer 2002;86: 819–27.
26. Raben D, Helfrich BA, Chan D, Johnson G, Bunn PA Jr. ZD1839, a selective epidermal growth factor receptor tyrosine kinase inhibitor, alone and in combination with radiation and chemotherapy as a new therapeutic strategy in non-small cell lung cancer. Semin Oncol 2002; 29:37–46.
27. Sirotnak FM, Zakowski MF, Miller VA, Scher HI, Kris MG. Efficacy of cytotoxic agents against human tumor xenografts is markedly enhanced by coadministration of ZD1839 (Iressa), an inhibitor of EGFR tyrosine kinase. Clin Cancer Res 2000;6:4885–92.
28. Williams KJ, Telfer BA, Stratford IJ, Wedge SR. ZD1839 ('Iressa'), a specific oral epidermal growth factor receptor-tyrosine kinase inhibitor, potentiates radiotherapy in a human colorectal cancer xenograft model. Br J Cancer 2002;86:1157–61.
29. Goldshmit Y, Erlich S, Pinkas-Kramarski R. Neuregulin rescues PC12-ErbB4 cells from cell death induced by H_2O_2. Regulation of reactive oxygen species levels by phosphatidylinositol 3-kinase. J Biol Chem 2001;276:46379–85.
30. Meves A, Stock SN, Beyerle A, Pittelkow MR, Peus D. H_2O_2 mediates oxidative stress-induced epidermal growth factor receptor phosphorylation. Toxicol Lett 2001;122:205–14.
31. Miyazaki Y, Hiraoka S, Tsutsui S, Kitamura S, Shinomura Y, Matsuzawa Y. Epidermal growth factor receptor mediates stress-induced expression of its ligands in rat gastric epithelial cells. Gastroenterology 2001;120:108–16.
32. Wang X, McCullough KD, Franke TF, Holbrook NJ. Epidermal growth factor receptor-dependent Akt activation by oxidative stress enhances cell survival. J Biol Chem 2000;275:14624–31.
33. Benhar M, Engelberg D, Levitzki A. Cisplatin-induced activation of the EGF receptor. Oncogene 2002;21:8723–31.
34. Kitagawa D, Tanemura S, Ohata S, Shimizu N, Seo J, Nishitai G, Watanabe T, Nakagawa K, Kishimoto H, Wada T, Tezuka T, Yamamoto T, et al. Activation of extracellular signal-regulated kinase by ultraviolet is mediated through Src-dependent epidermal growth factor receptor phosphorylation: its implication in an anti-apoptotic function. J Biol Chem 2002;277:366–71.

MUTATION IN BRIEF

Haplotypes of *CYP3A4* and Their Close Linkage With *CYP3A5* Haplotypes in a Japanese Population

Hiromi Fukushima-Uesaka[1], Yoshiro Saito[1]*, Hidemi Watanabe[1], Kisho Shiseki[1], Mayumi Saeki[1], Takahiro Nakamura[1], Kouichi Kurose[1], Kimie Sai[1], Kazuo Komamura[2,3], Kazuyuki Ueno[4], Shiro Kamakura[2], Masafumi Kitakaze[2], Sotaro Hanai[3], Toshiharu Nakajima[5], Kenji Matsumoto[5], Hirohisa Saito[5], Yu-ichi Goto[6], Hideo Kimura[6], Masaaki Katoh[7], Kenji Sugai[7], Narihiro Minami[6,7], Kuniaki Shirao[8], Tomohide Tamura[8], Noboru Yamamoto[8], Hironobu Minami[9], Atsushi Ohtsu[10], Teruhiko Yoshida[11], Nagahiro Saijo[8], Yutaka Kitamura[12,13], Naoyuki Kamatani[12], Shogo Ozawa[1], and Jun-ichi Sawada[1]

[1]Project Team for Pharmacogenetics, National Institute of Health Sciences, Tokyo, Japan; [2]Division of Cardiology, [3]Research Institute, [4]Department of Pharmacy, National Cardiovascular Center, Osaka, Japan; [5]Department of Allergy and Immunology, National Research Institute for Child Health and Development, National Center for Child Health and Development, Tokyo, Japan; [6]National Institute of Neuroscience, [7]National Center Hospital for Mental, Nervous and Muscular Disorders, National Center of Neurology and Psychiatry, Tokyo, Japan; [8]Division of Internal Medicine, National Cancer Center Hospital, [11]Genetics Division, National Cancer Center Research Institute, National Cancer Center, Tokyo, Japan; [9]Division of Oncology/Hematology, [10]Division of GI Oncology/Digestive Endoscopy, National Cancer Center Hospital East, Chiba, Japan; [12]Division of Genomic Medicine, Department of Advanced Biomedical Engineering and Science, Tokyo Women's Medical University, Tokyo, Japan; [13]Mitsubishi Research Institute, Inc., Tokyo, Japan

*Correspondence to: Yoshiro Saito, Project Team for Pharmacogenetics, National Institute of Health Sciences, 1-18-1, Kamiyoga, Setagaya-ku, Tokyo 158-8501, Japan; Tel.: +81-3-3700-9453; Fax: +81-3-5717-3832; E-mail: yoshiro@nihs.go.jp

Grant sponsor: Organization for Pharmaceutical Safety and Research of Japan; Grant numbers: MPJ-1, 2, 3, 5 and 6.

Communicated by Michael Dean

In order to identify single nucleotide polymorphisms (SNPs) and haplotype frequencies of *CYP3A4* in a Japanese population, the distal enhancer and proximal promoter regions, all exons, and the surrounding introns were sequenced from genomic DNA of 416 Japanese subjects. We found 24 SNPs, including 17 novel ones: two in the distal enhancer, four in the proximal promoter, one in the 5'-untranslated region (UTR), seven in the introns, and three in the 3'-UTR. The most common SNP was c.1026+12G>A (IVS10+12G>A), with a 0.249 frequency. Four non-synonymous SNPs, c.554C>G (p.T185S, *CYP3A4*16*), c.830_831insA (p.E277fsX8, **6*), c.878T>C (p.L293P, **18*), and c.1088 C>T (p.T363M, **11*) were found with frequencies of 0.014, 0.001, 0.028, and 0.002, respectively. No SNP was found in the known nuclear transcriptional factor-binding sites in the enhancer and promoter regions. Using these 24 SNPs, 16 haplotypes were unambiguously identified, and nine haplotypes were inferred by aid of an expectation-maximization-based program. In addition, using data

Received 17 July 2003; accepted revised manuscript 1 November 2003.

DOI: 10.1002/humu.9210

from 186 subjects enabled a close linkage to be found between *CYP3A4* and *CYP3A5* SNPs, especially among the SNPs at c.1026+12 in *CYP3A4* and c.219-237 (IVS3-237, a key SNP site for *CYP3A5*3*), c.865+77 (IVS9+77) and c.1523 in *CYP3A5*. This result suggested that *CYP3A4* and *CYP3A5* are within the same gene block. Haplotype analysis between *CYP3A4* and *CYP3A5* revealed several major haplotype combinations in the *CYP3A4-CYP3A5* block. Our findings provide fundamental and useful information for genotyping *CYP3A4* (and *CYP3A5*) in the Japanese, and probably Asian populations. © 2003 Wiley-Liss, Inc.

KEY WORDS: CYP3A4; CYP3A5; SNP; haplotype; Japanese

INTRODUCTION

The human cytochrome P450 (CYP) 3A subfamily has been estimated to be involved in the metabolism of half of the prescription drugs (Wrighton et al., 1996; Thummel and Wilkinson, 1998; Guengerich, 1999). The *CYP3A43* (MIM# 606534), *CYP3A4* (MIM# 124010), *CYP3A7* (MIM# 605340), and *CYP3A5* (MIM# 605325) genes consist of a cluster spanning 231 kb on chromosome 7 (Finta and Zaphiropoulos, 2000; Gellner et al., 2001). Among the family members, CYP3A4 is a predominant form in the adult human liver. CYP3A4 induction is mediated by pregnane/steroid X receptor (PXR), constitutive androstane receptor (CAR) and the vitamin D receptor by its binding to the distal xenobiotic-responsive enhancer module (XREM), especially to the distal nuclear receptor-binding element-1 (dNR1, imperfect DR-3 motif, -7733 to -7719 from the transcriptional start site) and dNR3 (imperfect DR-3 motif, -7290 to -7270 from the transcriptional start site), and to the proximal promoter region, especially to the proximal PXR response element (prPXRE, ER-6 motif, -169 to -152 from the transcriptional start site) (Goodwin et al., 1999, 2002; Drocourt et al., 2002). Recently, it has been reported that hepatic nuclear factor-4a (HNF-4a) also increases the activity of basal and a PXR/CAR-mediated reporter gene with the *CYP3A4* enhancer/promoter by its binding to the region immediately upstream of the dNR1 site in XREM (-7785 to -7772 from the transcriptional start site) (Tirona et al., 2003).

Up to 40-fold interindividual variations in CYP3A4 expression levels have been observed in the human liver. Furthermore, there is a 10-fold variation in the metabolism of CYP3A4 substrates *in vivo* (Thummel and Wilkinson, 1998; Guengerich, 1999). These interindividual differences are likely to be associated with efficacy and adverse effects of drugs. Thus, it is clinically important to predict CYP3A4 activity in the liver or other tissues, such as the intestine.

It has been suggested that approximately 85% of the interindividual variability in hepatic CYP3A4 activity is due to genetic factors (Ozdemir et al., 2000). Thus, several researches have focused on the identification of *CYP3A4* genetic variants (Lamba et al., 2002a). To date, 25 *CYP3A4* alleles (haplotypes), including 6 subtypes, have been publicized on the Human Cytochrome P450 Allele Nomenclature Committee homepage (www.imm.ki.se/CYPalleles). As for Caucasian populations, sequence-based genotyping was performed for 213 (Eiselt et al., 2001) and 53 (Lamba et al., 2002b) DNA samples. With Asian populations, however, only a PCR-SSCP analysis was performed with DNA samples from 102 Chinese subjects. In this report, 3 polymorphisms in the exons, including a frame-shift variant (*CYP3A4*6*), were identified by subsequent sequencing of variant samples found by PCR-SSCP (Hsieh et al., 2001). In other reports, only a small number of samples (24 or 30) were sequenced (Dai et al., 2001; Lamba et al., 2002b). Thus, there has been no comprehensive sequence analysis of *CYP3A4* for Asian populations, including the Japanese. Furthermore, there has been no report on *CYP3A4* haplotype analysis for any population. Increasingly, association studies have shown that haplotypes, linked combinations of SNPs, have the advantage of giving more precise detection of the phenotype-genotype link than do the individual SNPs (Judson et al., 2000). Therefore, in order to identify SNPs and haplotypes in the Japanese, we sequenced the distal enhancer region (-7989 to -7114 from the translational start codon, corresponding to -7886 to -7011 from the transcriptional start site), the proximal promoter region (up to 913 basepairs upstream of the translational start codon, corresponding to up to -810 from the transcriptional start site), all the exons, and the surrounding intronic regions of *CYP3A4* for 416 Japanese individuals. Then, linkage disequilibrium analysis was performed for the *CYP3A4* and *CYP3A5* genes together, using the data from 186 identical subjects described in the previous report (Saeki et al., 2003). Strong linkage was found between the SNPs in these two genes. Therefore, we further inferred haplotype combinations of the region covering *CYP3A4* and *CYP3A5*.

METHODS

Human genomic DNA samples

All 416 Japanese subjects were either patients with arrhythmia who were administered anti-arrhythmic drugs, cancer patients who were administered irinotecan or paclitaxel, patients with epilepsy who were administered anti-epileptic drugs, or patients with allergic diseases (atopic dermatitis and/or asthma) who were administered steroidal drugs. Genomic DNA was extracted directly from blood leukocytes (343 samples) or from lymphocytes immortalized with the Epstein-Barr virus (73 samples). This study was approved by the ethical review boards of the National Cardiovascular Center, the National Cancer Center, the National Center of Neurology and Psychiatry, the National Center for Child Health and Development, and the National Institute of Health Sciences. Written informed consent was obtained from all subjects.

Polymerase chain reaction (PCR) conditions and DNA sequencing

First, the entire *CYP3A4* gene (GenBank Accession # AF280107.1) was amplified in 3 amplicons: the distal enhancer region to exon 2, the proximal promoter region to exon 7, and exons 5 to 13. The primer sequences can be obtained by a request to the corresponding author. Genomic DNA (150 ng) was amplified using 1.25 units of *Z*-Taq (Takara Shuzo, Tokyo, Japan) with 0.2 μM primers. The first-round PCR was 30 cycles of 5 sec at 98°C, 5 sec at 55°C, and 190 sec at 72°C. Next, the promoter region and each exon were amplified by *Ex*-Taq (0.625 units) (Takara Shuzo) with the appropriate sets of *CYP3A4*-specific primers (0.5 μM). Second-round PCR consisted of 5 min at 94°C, followed by 30 cycles of 30 sec at 94°C, 1 min at 55°C, and 2 min at 72°C, and then a final extension for 5 min at 72°C. The PCR products were treated with the PCR Product Pre-Sequencing Kit (USB Co., Cleveland, OH) and directly sequenced on both strands using the ABI BigDye Terminator Cycle Sequencing Kit (version 3, Applied Biosystems, Foster City, CA). The primers for the second round PCR were also used for sequencing, except for the distal enhancer region and exons 1, 2, 4, 11, and 12. Excess dye was removed with a DyeEx96 kit (Qiagen, Hilden, Germany), and the eluates were analyzed on an ABI Prism 3700 or 3730 DNA Analyzer (Applied Biosystems). Conditions for PCR and *CYP3A5* (GenBank Accession # NG_000004.2) sequencing were described previously (Saeki et al., 2003). The amplification and sequencing of *CYP3A7* (GenBank Accession # AF280107.1) promoter region were performed according to Kuehl et al. (2001). All the SNPs were confirmed by repeating the PCR on genomic DNA and sequencing the newly generated PCR products.

Haplotype analysis

Some of the haplotypes were unambiguous from subjects with homozygous SNPs at all sites or a heterozygous SNP at only one site, and will be publicized on the Human Cytochrome P450 Allele Nomenclature Committee homepage. Separately, the diplotype configurations (a combination of haplotypes) were inferred by LDSUPPORT software, which determines the posterior probability distribution of the diplotype configuration for each subject based on the estimated haplotype frequencies (Kitamura et al., 2002). Linkage analysis was performed by SNPAlyze software (Dynacom Co., Yokohama, Japan). Nucleotide diversity (π) was calculated using DnaSP software (Rozas and Rozas, 1999).

RESULTS

The distal enhancer region, proximal promoter region, all exons, and surrounding intronic regions of *CYP3A4* for 416 Japanese subjects were sequenced. Twenty-four SNPs, including 17 novel ones [2 were in the distal enhancer region, 4 in the proximal promoter region, 1 in the 5'-untranslated region (UTR), 7 in the introns and 3 in the 3'-UTR] were detected (see Table 1). All of the allelic frequencies were in the Hardy-Weinberg equilibrium (p>0.387 or higher). Since we did not find apparent differences in SNP frequencies among the subjects with the different disease types (data not shown), the data for all subjects were analyzed as one group. The most common SNP was c.1026+12G>A (IVS10+12G>A) with a 0.249 frequency.

Table 1 Diplotype configulation of *CYP3A4*

Exon/Intron		Enhancer	Enhancer	Promoter	Promoter	Promoter	Promoter	5'-UTR	Intron 1	Intron 3	Intron 5	Intron 6	Exon 7	Intron 7	Intron 7	Intron 7	Exon 9	Intron 9	Intron 9	Exon 10	Intron 10	Exon 11	3'-UTR	3'-UTR	3'-UTR	Number of subjects	
Position on AF280107.1		g.54133	g.54436	g.61371	g.61382	g.61407	g.61588	g.61971	g.65993	g.68113	g.76236	g.77589	g.77639	g.77763	g.77845	g.78811	g.79697_79698	g.79754	g.79851_79852	g.82106	g.82266	g.83903	g.84049	g.84049	g.88242		
cDNA change[1]		c.-7904 C>A	c.-7681 delA	c.-666 C>A	c.-655 A>G	c.-630 A>C	c.-156 C>A	c.-66 C>G	c.72-41 delA	c.218+22 A>G	c.433-17 T>G	c.522-18 A>C	c.554 C>G	c.670+8 G>A	c.678+90 T>C	c.671-40 A>G	c.830_831 insA	c.865+22 G>A	c.865+119_120 delAT	c.878 T>C	c.1026+12 G>A	c.1088 C>T	c.1585 T>G	c.1585 T>C	c.1778 C>A		
Amino acid change													p.T185S				p.E277fsX8			p.L293P		p.T363M					
Reference		Novel	Novel	Novel	Novel	Novel	Novel	Novel	Novel	Novel	Dai et al., (2001)	Novel	*16	Novel	Novel	Novel	*6	Novel	Dai et al., (2001)	*18	Dai et al., (2001)	*11	Novel	Novel	Novel		
Diplotype[2]	*1A/*1A																									224	381
	*1G/*1A																									107	
	*1H/*1A																									3	
	*1K/*1A																									1	
	*1L/*1A																									1	
	*1M/*1A																									1	
	*1N/*1A																									3	
	*1P/*1A																									1	
	*1Q/*1A																									1	
	*1R/*1A																									1	
	*1S/*1A																									1	
	*1T/*1A																									1	
	*1H/*1A																									5	
	*1a/*1A																									1	
	*1w/*1A																									1	
	*1m/*1A																									1	
	*1o/*1A																									1	
	*1p/*1A																									1	
	*1z/*1A																									1	
	*1aa/*1A																									1	
	*1G/*1G																									21	
	*1H/*1G																									3	
	*6/*1A																									1	35 (amino acid change)
	*11b/*1A																									1	
	*16b/*1A																									9	
	*18b/*1A																									17	
	*16B/*1G																									1	
	*11c/*1G																									1	
	*18B/*1A																									3	
	*16B/*18b																									1	
	*18B/*18B																									1	
SNP frequency		0.001	0.001	0.001	0.001	0.001	0.001	0.001	0.001	0.004	0.001	0.001	0.014	0.001	0.001	0.001	0.001	0.001	0.001	0.028	0.249	0.002	0.001	0.001	0.010	416	

Haplotype[2]		Frequency
	*1A	0.734
	*1G	0.189
	*1H	0.010
	*1J	0.004
	*1K	0.001
	*1L	0.001
	*1M	0.001
	*1N	0.001
	*1P	0.001
	*1Q	0.001
	*1R	0.001
	*1S	0.001
	*1T	0.001
	*1u	0.001
	*1v	0.001
	*1w	0.001
	*1x	0.001
	*1y	0.001
	*1z	0.001
	*1aa	0.001
	*6	0.001
	*11b	0.001
	*11c	0.001
	*16B	0.014
	*18B	0.028

[1]Position on the cDNA sequence (A of the translational start codon is 1, based on GenBank Accession # AF280107.1) or position from the end of the nearest exon.

[2]White cell, wild-type; gray cell, heterozygous alteration; black cell, homozygous alteration. The unambiguously assigned haplotypes approved by Human Cytochrome P450 Allele Nomenclature Committee are described by using capital alphabetical letters.

Table 2: Haplotype Combinations of CYP3A4 and CYP3A5

Haplotype combination (CYP3A4-CYP3A5)	Frequency
*1A-*3A	.696
*1G-*1E	.120
*18B-*1E	.027
*1A-*3C	.022
*1A-*3F#	.022
*1G-*3A	.019
*1A-*1E	.019
*16B-*1E	.016
*1G-*1f	.014
*1G-*1g	.005
*1H-*1g	.005
*11c-*1E	.003
*1A-*1h	.003
*1A-*3H#	.003
*1A-*3i	.003
*1A-*3J#	.003
*1aa-*1E	.003
*1G-*3C	.003
*1G-*3G#	.003
*1H-*1E	.003
*1M-*3F#	.003
*1S-*3C	.003
*1v-*1i	.003
*1w-*3A	.003

#The haplotypes *CYP3A5*3F*, **3G*, **3H* and **3J*, published in the Human Cytochrome P450 Allele Nomenclature Committee homepage, were formally described as **3d*, **3e*, **3f* and **3h* in our previous paper (Saeki et al., 2003).

As for the SNPs identified in the exons, 4 reported non-synonymous SNPs were detected: c.554C>G (p.T185S, *CYP3A4*16*), c.830_831insA (p.E277fsX8, resulting in an early stop codon TGA at 285, **6*), c.878T>C (p.L293P, **18*), and c.1088 C>T (p.T363M, **11*) with frequencies of 0.014, 0.001, 0.028, and 0.002, respectively (Table 1). *CYP3A4*16* or **18* was always detected together with the SNP, c.1026+12G>A.

Two novel SNPs were found in the distal enhancer regions. The positions are 16 bases upstream of the HNF-4a binding motif and 221 bases downstream of dNR-1. Also, four novel SNPs were detected in the proximal promoter regions, but these were at least 100 bases from prPXRE. The functional influence of the non-coding SNPs, located in the 5'-UTR, introns, and 3'-UTR, is currently unknown. The calculated nucleotide diversity (π) using all samples was 0.00008.

Using the detected SNPs in *CYP3A4*, haplotype analysis was then performed. Some haplotypes were first unambiguously assigned by homozygous SNPs at all sites (**1G* and **18B*) or a heterozygous SNP at only one site (**1H-*1T* and **16B*). They are described in capital alphabetical letters in Table 1 (These haplotypes will be publicized on the Human Cytochrome P450 Allele Nomenclature Committee homepage). Separately, we estimated the diplotype configuration (a combination of haplotypes) for each subject by LDSUPPORT software. The diplotype configurations of all the subjects had a probability (certainty) of >99.99%. The additionally inferred haplotypes were seven **1* subtypes (**1u-*1aa*) and two **11* subtypes (**11b and *11c*) (Table 1). The most frequent haplotype was **1A* (frequency: 0.734), followed by **1G* (0.189), **18B* (0.028), **16B* (0.014), and **1H* (0.010). The frequencies of the other haplotypes were less than 0.01.

In addition to *CYP3A4* haplotypes, we previously identified *CYP3A5* haplotypes, another *CYP3A* family gene with a polymorphic expression pattern (Saeki et al., 2003). Using the data from 186 subjects (also included in this study), linkage disequilibrium analysis was performed with the SNPs of *CYP3A4* and *CYP3A5* simultaneously.

The most frequent SNP in *CYP3A4*, c.1026+12G>A, showed a strong linkage with c.219-237A>G (IVS3-237A>G) inversely (namely G>A; *CYP3A5*3*, Kuehl et al., 2001) [ρ^2 = 0.722 and Chi^2 = 271.0 (p<0.0001)], c.865+77G>T [ρ^2 = 0.638 and Chi^2 = 241.0 (p<0.0001)] and c.1523C>T inversely [ρ^2 = 0.606 and Chi^2 = 221.3 (p<0.0001)] in *CYP3A5*. In other words, c.1026+12G (wild type) in *CYP3A4* is linked to c.219-237G and c.1523T (**3A*) in *CYP3A5*. These three SNPs in *CYP3A5* also showed a weak linkage with the SNP at c.554 (**16*) or c.878 (**18*) in *CYP3A4*. These results suggested that *CYP3A4* and *CYP3A5* are within the same gene block.

Then, we further inferred combinations of *CYP3A4* and *CYP3A5* haplotypes utilizing LDSUPPORT software (Table 2). Using the data with the probability (certainty) over 0.98 from 184 subjects, we calculated the frequencies of haplotype combinations in the *CYP3A4-3A5* block (Table 2). The most frequent combination (*CYP3A4-CYP3A5*) was **1A-*3A* (frequency: 0.696), followed by **1G-*1E* (0.120), **18B-*1E* (0.027), **1A-*3C* (0.022), and **1A-*3F* (0.022). The frequencies of the other haplotypes were less than 0.02.

CYP3A7 is known as a fetal form of CYP3A, but has been reported to be expressed in 14 out of 15 Japanese adult subjects (Tateishi et al., 1999). We also searched for *CYP3A7*1B and *1C*, which were shown to be the main polymorphisms responsible for *CYP3A7* expression in Caucasian adult livers (Burk et al., 2002), but could not detect these polymorphisms in 268 samples (data not shown). Instead, we detected an SNP c.–425G>C (A of the translational start site for *CYP3A7* is numbered +1, rs3823647 in the dbSNP database) in this area with a 0.011 frequency, and found a perfect linkage between this SNP and *CYP3A5*1f* SNPs (c.166-102C>T and c.1253+177C>T) [ρ^2 = 1.00 and Chi^2 = 340 (p<0.0001)] using data from 170 samples (Saeki et al., 2003).

DISCUSSION

Here, we report the screening of *CYP3A4* SNPs in a Japanese population. Overall, we detected 17 novel and 7 known SNPs, including four non-synonymous ones (Table 1). *CYP3A4*11* (p.T363M) and **16* (p.T185S) have reduced *in vitro* catalytic activities against testosterone with lowered protein expression levels (Eiselt et al., 2001; Murayama et al., 2002). *CYP3A4*6* (p.E277fsX8) was found in a patient with a lowered urinary 6ß-hydroxycortisol to free cortisol ratio, suggesting decreased CYP3A4 activity (Hsieh et al., 2001). On the other hand, *CYP3A4*18* (p.L293P) induced unchanged or rather increased activity to testosterone and chlorpyrifos *in vitro* (Dai et al., 2001; Murayama et al., 2002). The subjects with these non-synonymous SNPs (total frequency: 0.045) may have an altered CYP3A4 activity.

Large ethnic differences in *CYP3A4* SNPs have been reported, such as *CYP3A4*1B* (c.-392A>G), which has been detected in 9% of Caucasians, 53% of Africans, and no Asians (Walker et al., 1998). As for SNPs located in the exons, p.M445T (**3*) and p.F189S (**17*) were only found in Caucasians, p.R162Q (**15*) was in Africans, and p.D174H (**10*) were in both Caucasians and Africans (Dai et al., 2001; Lamba et al., 2002b). Of the SNPs detected in this study, **6* was previously found in the Chinese, **16* in Mexicans and the Japanese, and **18* in the Chinese (Hsieh et al., 2001; Dai et al., 2001; Lamba et al., 2002b). These ethnic differences of the SNPs also imply haplotype differences. We found 25 haplotypes, including 16 unambiguous ones. However, no detailed haplotypes have been reported in other ethnic populations. Comparable studies should be done in the future.

In the following order, *CYP3A43*, *CYP3A4*, *CYP3A7*, and *CYP3A5*, are in a gene cluster spanning 231 kb on chromosome 7. This study also showed that a close linkage between *CYP3A4* and *CYP3A5* SNPs, especially among the SNPs at c.1026+12 in *CYP3A4*, and c.219-237 (a key SNP site for *CYP3A5*3*), c.865+77 and c.1523 in *CYP3A5*. c.1026+12 in *CYP3A4* is approximately 91 kb from c.219-237 in *CYP3A5* and 116 kb from c.1523 in *CYP3A5*. c.219-237A>G in *CYP3A5* induces aberrant splicing, resulting in defective activity (Kuehl et al., 2001).

Since CYP3A4 and CYP3A5 largely metabolize the same substrates, it is worth analyzing the haplotype combinations (Table 2). Major combinations (*CYP3A4-3A5*) were **1A-*3A* and **1G-*1E*. Our previous study showed that *CYP3A5*3* was the predominant defective allele in a Japanese population (Saeki et al., 2003). According to the obtained haplotype combinations, the *CYP3A4* haplotypes containing the c.1026+12G allele (such as **1A*) are linked to *CYP3A5*3* with a 97% probability. Inversely, 88% of the *CYP3A4* haplotypes with c.1026+12A (such as **1G*) are linked to *CYP3A5*1*. Thus, these results suggested that genotyping at the IVS10+12 position in *CYP3A4* can predict if the subject has *CYP3A5*3* in a Japanese population. In addition, the activity-decreasing haplotype *CYP3A4*16B* perfectly linked with *CYP3A5*1E*, but not **3*, suggesting that the resulting expression of CYP3A5 can compensate for decreased CYP3A4 activity. Recently, the importance of

haplotype analysis has been shown in phenotype-genotype association studies as well as candidate gene discovery (Judson et al., 2000). Our data also demonstrate the usefulness of haplotype analysis for the prediction of total CYP3A activity. The haplotype combination analysis should include *CYP3A7* haplotypes in the future.

In conclusion, we assigned *CYP3A4* haplotypes and showed its close linkage with *CYP3A5* haplotypes. The assigned haplotypes provide fundamental and useful information for genotyping *CYP3A4* and *CYP3A5* in the Japanese, and probably the Asian populations.

ACKNOWLEDGMENTS

The authors, Hiromi Fukushima-Uesaka and Yoshiro Saito, contributed equally to this work. We would like to thank Mr. Jyoji Kamimura (CTC Laboratory Systems Corp.) for his generous support.

REFERENCES

Burk O, Tegude H, Koch I, Hustert E, Wolbold R, Glaeser H, Klein K, Fromm MF, Nuessler AK, Neuhaus P, Zanger UM, Eichelbaum M, Wojnowski L. 2002. Molecular mechanisms of polymorphic *CYP3A7* expression in adult human liver and intestine. J Biol Chem 277:24280-24288.

Dai D, Tang J, Rose R, Hodgson E, Bienstock RL, Mohrenweiser HW, Goldstein JA. 2001. Identification of variants of CYP3A4 and characterization of their abilities to metabolize testosterone and chlorpyrifos. J Pharmacol Exp Ther 299:825-831.

Drocourt L, Ourlin JC, Pascussi JM, Maurel P, Vilarem MJ. 2002. Expression of *CYP3A4*, *CYP2B6*, and *CYP2C9* is regulated by the vitamin D receptor pathway in primary human hepatocytes. J Biol Chem 277:25125-25132.

Eiselt R, Domanski TL, Zibat A, Mueller R, Presecan-Siedel E, Hustert E, Zanger UM, Brockmoller J, Klenk H, Meyer UA, Khan KK, He Y, Halpert JR, Wojnowski L. 2001. Identification and functional characterization of eight CYP3A4 protein variants. Pharmacogenetics 11:447-458.

Finta C, Zaphiropoulos PG. 2000. The human cytochrome P450 3A locus. Gene evolution by capture of downstream exons. Gene 260:13-23.

Gellner K, Eiselt R, Hustert E, Arnold H, Koch I, Haberl M, Deglmann CJ, Burk O, Buntefuss D, Escher S, Bishop C, Koebe HG, Brinkmann U, Klenk HP, Kleine K, Meyer UA, Wojnowski L. 2001. Genomic organization of the human *CYP3A* locus: identification of a new, inducible *CYP3A* gene. Pharmacogenetics 11:111-121.

Goodwin B, Hodgson E, Liddle C. 1999. The orphan human pregnane X receptor mediates the transcriptional activation of *CYP3A4* by rifampicin through a distal enhancer module. Mol Pharmacol 56:1329-1339.

Goodwin B, Hodgson E, D'Costa DJ, Robertson GR, Liddle C. 2002. Transcriptional regulation of the human *CYP3A4* gene by the constitutive androstane receptor. Mol Pharmacol 62:359-365.

Guengerich FP. 1999 Cytochrome P-450 3A4: regulation and role in drug metabolism. Annu Rev Pharmacol Toxicol 39:1-17.

Hsieh KP, Lin YY, Cheng CL, Lai ML, Lin MS, Siest JP, Huang JD. 2001. Novel mutations of CYP3A4 in Chinese. Drug Metab Dispos 29:268-273.

Judson R, Stephens JC, Windemuth A. 2000. The predictive power of haplotypes in clinical response. Pharmacogenomics, 1: 15-26.

Kitamura Y, Moriguchi M, Kaneko H, Morisaki H, Morisaki T, Toyama K, Kamatani N. 2002. Detèrmination of probability distribution of diplotype configulation (diplotype distribution) for each subject from genotypic data using the EM algorithm. Ann Hum Genet 66:183-193.

Kuehl P, Zhang J, Lin Y, Lamba J, Assem M, Schuetz J, Watkins PB, Daly A, Wrighton SA, Hall SD, Maurel P, Relling M, Brimer C, Yasuda K, Venkataramanan R, Strom S, Thummel K, Boguski MS, Schuetz E. 2001. Sequence diversity in *CYP3A* promoters and characterization of the genetic basis of polymorphic CYP3A5 expression. Nat Genet 27:383-391.

Lamba JK, Lin YS, Schuetz EG, Thummel KE. 2002a Genetic contribution to variable human CYP3A-mediated metabolism. Adv Drug Deliv Rev 54:1271-1294.

Lamba JK, Lin YS, Thummel K, Daly A, Watkins PB, Strom S, Zhang J, Schuetz EG. 2002b. Common allelic variants of cytochrome P4503A4 and their prevalence in different populations. Pharmacogenetics 12:121-132.

Murayama N, Nakamura T, Saeki M, Soyama A, Saito Y, Sai K, Ishida S, Nakajima O, Itoda M, Ohno Y, Ozawa S, Sawada J. 2002. *CYP3A4* gene polymorphisms influence testosterone 6a-hydroxylation. Drug Metabol Pharmacokin 17:150-156.

Ozdemir V, Kalow W, Tang BK, Paterson AD, Walker SE, Endrenyi L, Kashuba AD. 2000. Evaluation of the genetic component of variability in CYP3A4 activity: a repeated drug administration method. Pharmacogenetics 10:373-388.

Rozas J, Rozas R. 1999. DnaSP version 3: an integrated program for molecular population genetics and molecular evolution analysis. Bioinformatics 15:174-175.

Saeki M, Saito Y, Nakamura T, Murayama N, Kim SR, Ozawa S, Komamura K, Ueno K, Kamakura S, Nakajima T, Saito H, Kitamura Y, Kamatani N, Sawada J. 2003. Single nucleotide polymorphisms (SNPs) and haplotype frequencies of *CYP3A5* in a Japanese population. Hum Mut 21:653 (Mutation in Brief #618).

Tateishi T, Watanabe M, Moriya H, Yamaguchi S, Sato T, Kobayashi S. 1999. No ethnic difference between Caucasian and Japanese hepatic samples in the expression frequency of CYP3A5 and CYP3A7 proteins. Biochem Pharmacol. 57:935-939.

Tirona RG, Lee W, Leake BF, Lan LB, Cline CB, Lamba V, Parviz F, Duncan SA, Inoue Y, Gonzalez FJ, Schuetz EG, Kim RB 2003. The orphan nuclear receptor HNF4a determines PXR- and CAR-mediated xenobiotic induction of CYP3A4. Nat Med 9:220-224.

Thummel KE, Wilkinson GR. 1998. In vitro and in vivo drug interactions involving human CYP3A. Annu Rev Pharmacol Toxicol 38:389-430.

Walker AH, Jaffe JM, Gunasegaram S, Cummings SA, Huang CS, Chern HD, Olopade OI, Weber BL, Rebbeck TR. 1998, Characterization of an allelic variant in the nifedipine-specific element of CYP3A4: ethnic distribution and implications for prostate cancer risk. Hum Mutat 12:289 (Mutation in Brief #191).

Wrighton SA, VandenBranden M, Ring BJ. 1996. The human drug metabolizing cytochromes P450. J Pharmacokinet Biopharm 24:461-473.

VOLUME 23 · NUMBER 6 · FEBRUARY 20 2005

JOURNAL OF CLINICAL ONCOLOGY

ORIGINAL REPORT

Randomized Pharmacokinetic and Pharmacodynamic Study of Docetaxel: Dosing Based on Body-Surface Area Compared With Individualized Dosing Based on Cytochrome P450 Activity Estimated Using a Urinary Metabolite of Exogenous Cortisol

Noboru Yamamoto, Tomohide Tamura, Haruyasu Murakami, Tatsu Shimoyama, Hiroshi Nokihara, Yutaka Ueda, Ikuo Sekine, Hideo Kunitoh, Yuichiro Ohe, Tetsuro Kodama, Mikiko Shimizu, Kazuto Nishio, Naoki Ishizuka, and Nagahiro Saijo

From the Division of Internal Medicine, National Cancer Center Hospital; Pharmacology Division and Cancer Information and Epidemiology Division, National Cancer Center Research Institute, Tokyo, Japan.

Submitted November 7, 2003; accepted August 19, 2004.

Supported in part by a Grant-in-Aid for Cancer Research (9-25) from the Ministry of Health, Labor, and Welfare, Tokyo, Japan.

Presented in part at the 38th Annual Meeting of the American Society of Clinical Oncology, May 18-21, 2002, Orlando, FL.

Authors' disclosures of potential conflicts of interest are found at the end of this article.

Address reprint requests to Tomohide Tamura, MD, Division of Internal Medicine, National Cancer Center Hospital, 5-1-1, Tsukiji, Chuo-ku, Tokyo, 104-0045, Japan; e-mail: ttamura@ncc.go.jp.

0732-183X/05/2306-1061/$20.00

DOI: 10.1200/JCO.2005.11.036

ABSTRACT

Purpose

Docetaxel is metabolized by cytochrome P450 (CYP3A4) enzyme, and the area under the concentration-time curve (AUC) is correlated with neutropenia. We developed a novel method for estimating the interpatient variability of CYP3A4 activity by the urinary metabolite of exogenous cortisol (6-beta-hydroxycortisol [6-β-OHF]). This study was designed to assess whether the application of our method to individualized dosing could decrease pharmacokinetic (PK) and pharmacodynamic (PD) variability compared with body-surface area (BSA) –based dosing.

Patients and Methods

Fifty-nine patients with advanced non–small-cell lung cancer were randomly assigned to either the BSA-based arm or individualized arm. In the BSA-based arm, 60 mg/m^2 of docetaxel was administered. In the individualized arm, individualized doses of docetaxel were calculated from the estimated clearance (estimated clearance = 31.177 + [7.655 × 10^{-4} × total 6-β-OHF] − [4.02 × alpha-1 acid glycoprotein] − [0.172 × AST] − [0.125 × age]) and the target AUC of 2.66 mg/L · h.

Results

In the individualized arm, individualized doses of docetaxel ranged from 37.4 to 76.4 mg/m^2 (mean, 58.1 mg/m^2). The mean AUC and standard deviation (SD) were 2.71 (range, 2.02 to 3.40 mg/L · h) and 0.40 mg/L · h in the BSA-based arm, and 2.64 (range, 2.15 to 3.07 mg/L · h) and 0.22 mg/L · h in the individualized arm, respectively. The SD of the AUC was significantly smaller in the individualized arm than in the BSA-based arm ($P < .01$). The percentage decrease in absolute neutrophil count (ANC) averaged 87.1% (range, 59.0 to 97.7%; SD, 8.7) in the BSA-based arm, and 87.4% (range, 78.0 to 97.2%; SD, 6.1) in the individualized arm, suggesting that the interpatient variability in percent decrease in ANC was slightly smaller in the individualized arm.

Conclusion

The individualized dosing method based on the total amount of urinary 6-β-OHF after cortisol administration can decrease PK variability of docetaxel.

J Clin Oncol 23:1061-1069. © 2005 by American Society of Clinical Oncology

INTRODUCTION

Many cytotoxic drugs have narrow therapeutic windows despite having a large interpatient pharmacokinetic (PK) variability. The doses of these cytotoxic drugs are usually calculated on the basis of body-surface area (BSA). Although several physiologic functions are proportional to BSA, systemic exposure to a drug is only partially related to

this parameter.[1-3] Consequently, a large interpatient PK variability is seen when doses are based on BSA. This large interpatient PK variability can result in undertreatment with inappropriate therapeutic effects in some patients, or in overtreatment with unacceptable severe toxicities in others. Understanding interpatient PK variability is important for optimizing anticancer treatments. Factors that affect PK variability include drug absorption, metabolism, and excretion. Among these factors, drug metabolism is regarded as a major factor causing PK variability. Unfortunately, however, no simple and practical method for estimating the interpatient variability of drug metabolism is available. If drug metabolism in each patient could be predicted, individualized dosing could be performed to optimize drug exposure while minimizing unacceptable toxicity.

Docetaxel is a cytotoxic agent that promotes microtubule assembly and inhibits depolymerization to free tubulin, resulting in the blockage of the M phase of the cell cycle.[4] Docetaxel has shown promising activity against several malignancies, including non–small-cell lung cancer, and is metabolized by hepatic CYP3A4 enzyme.[5-15]

Human CYP3A4 is a major cytochrome P450 enzyme that is present abundantly in human liver microsomes and is involved in the metabolism of a large number of drugs, including anticancer drugs.[16-18] This enzyme exhibits a remarkable interpatient variation in activity as high as 20-fold, which accounts for the large interpatient differences in the disposition of drugs that are metabolized by this enzyme.[19-22] Several noninvasive in vivo probes for estimating the interpatient variability of CYP3A4 activity have been reported and include the erythromycin breath test, the urinary dapsone recovery test, measurement of midazolam clearance (CL), and measurement of the ratio of endogenous urinary 6-beta-hydroxycortisol (6-β-OHF) to free-cortisol (FC).[23-27] The erythromycin breath test and the measurement of midazolam CL are the best validated, and both have been shown to predict docetaxel CL in patients.[28,29] However, neither probe has been used in a prospective study to validate the correlations observed, or to test their utility in guiding individualized dosing.

We developed a novel method for estimating the interpatient variability of CYP3A4 activity by urinary metabolite of exogenous cortisol. The total amount of 24-hour urinary 6-β-OHF after cortisol administration (total 6-β-OHF) is significantly correlated with docetaxel CL, which is metabolized by the CYP3A4 enzyme. We also illustrate the possibility that individualized dosing to optimize drug exposure and decrease interpatient PK variability could be performed using this method.[30]

We conducted a prospective, randomized PK and pharmacodynamic (PD) study of docetaxel comparing BSA-based dosing and individualized dosing based on the interpatient variability of CYP3A4 activity, as estimated by a urinary metabolite of exogenous cortisol. The objective of this study was to assess whether the application of our method to individualized dosing could decrease PK and PD variability of docetaxel compared with BSA-based dosing.

PATIENTS AND METHODS

Patient Selection

Patients with histologically or cytologically documented advanced or metastatic non–small-cell lung cancer were eligible for this study. Other eligibility criteria included the following: age $\geq$ 20 years; Eastern Cooperative Oncology Group performance status of 0, 1, or 2; 4 weeks of rest since any previous anticancer therapy; and adequate bone marrow (absolute neutrophil count [ANC] $\geq$ 2,000/μL and platelet count $\geq$ 100,000/μL), renal (serum creatinine level $\leq$ 1.5 mg/dL), and hepatic (serum total bilirubin level $\leq$ 1.5 mg/dL, AST level $\leq$ 150 U/L, and ALT level $\leq$ 150 U/L) function. Written informed consent was obtained from all patients before enrollment onto the study.

The exclusion criteria included the following: pregnancy or lactation; concomitant radiotherapy for primary or metastatic sites; concomitant chemotherapy with any other anticancer agents; treatment with steroids or any other drugs known to induce or inhibit CYP3A4 enzyme[17]; serious pre-existing medical conditions, such as uncontrolled infections, severe heart disease, diabetes, or pleural or pericardial effusions requiring drainage; and a known history of hypersensitivity to polysorbate 80. This study was approved by the institutional review board of the National Cancer Center.

Pretreatment and Follow-Up Evaluation

On enrollment onto the study, a history and physical examination were performed, and a complete differential blood cell count (including WBC count, ANC, hemoglobin, and platelets), and a clinical chemistry analysis (including serum total protein, albumin [ALB], bilirubin, creatinine, AST, ALT, gamma-glutamyltransferase, alkaline phosphatase [ALP], and alpha-1 acid glycoprotein [AAG]) were performed. Blood cell counts and a chemistry analysis except for AAG were performed at least twice a week throughout the study. Tumor measurements were performed every two cycles, and antitumor response was assessed by WHO standard response criteria. Toxicity was evaluated according to the National Cancer Institute Common Toxicity Criteria (version 2.0).

Study Design

This study was designed to assess whether the application of our method to individualized dosing could decrease PK and PD variability compared with BSA-based dosing. The primary end point was PK variability and the secondary end point was PD variability (ie, toxicity). In our previous study involving 29 patients who received 60 mg/m^2 of docetaxel, the area under the concentration-time curve (AUC) was calculated to be 2.66 $\pm$ 0.91 (mean $\pm$ standard deviation [SD]) mg/L $\cdot$ h.[30] We assumed that the variability of AUC, represented by the SD, could be reduced by 50% in the individualized arm compared with that in the BSA-based arm, and that AUC would be normally distributed. The required sample size was 25 patients per arm to detect this difference with a two-sided F test at α = .05 and a power of 0.914.

Patients were randomly assigned to either the BSA-based arm or individualized arm (Fig 1). In the BSA-based arm, each patient received a dose of 60 mg/m^2 of docetaxel. In the individualized arm, individualized doses of docetaxel were calculated from the estimated docetaxel CL after cortisol administration and the target AUC (described in the Docetaxel Administration section).

Cortisol Administration and Urine Collection

In the individualized arm, 300 mg of hydrocortisone (Banyu Pharmaceuticals Co, Tokyo, Japan) was diluted in 100 mL of 0.9%

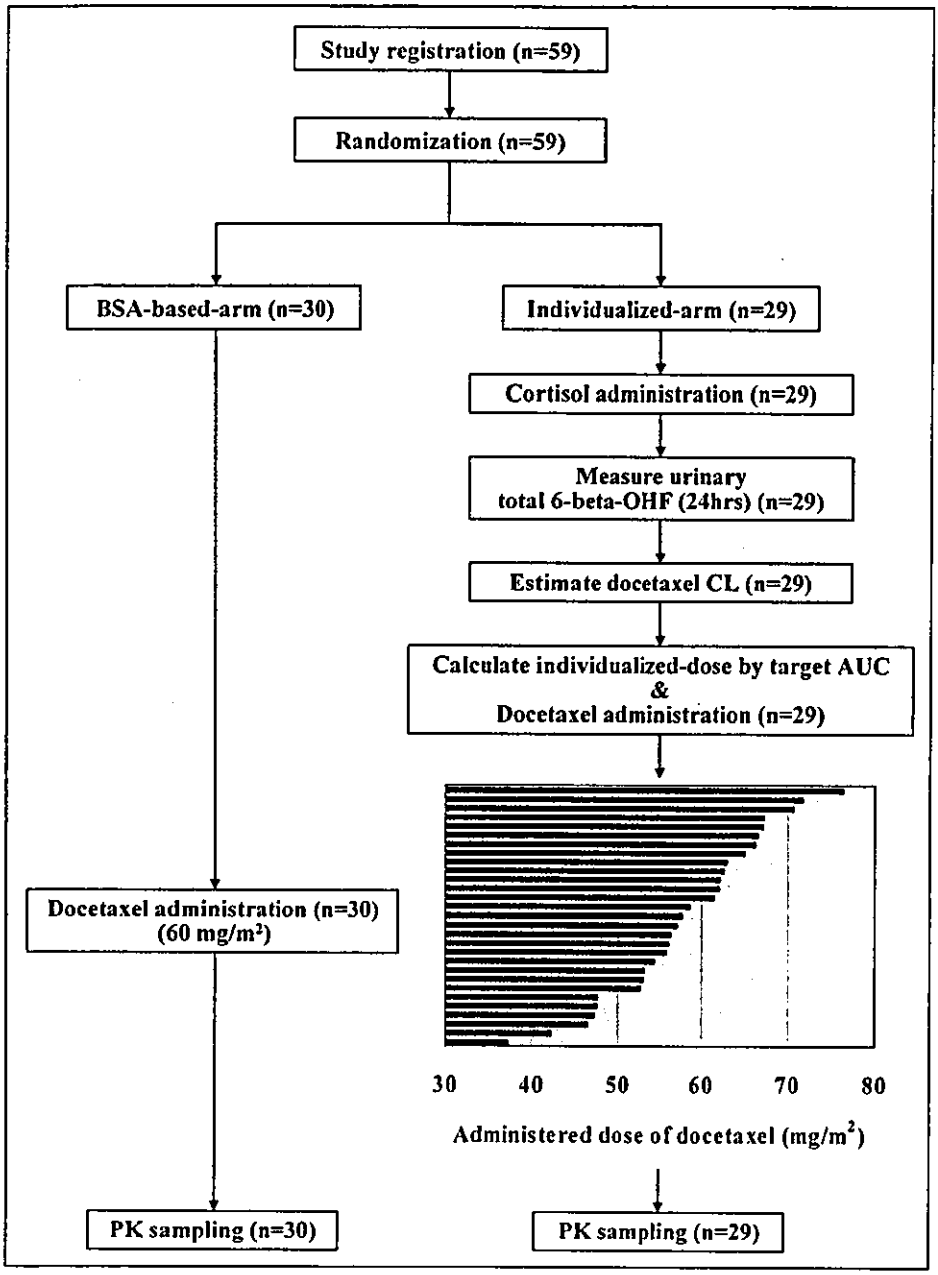

Fig 1. Study flow diagram and administered dose of docetaxel. PK, pharmacokinetic; AUC, area under the concentration-time curve; CL, clearance; 6-β-OHF, 6-beta-hydroxycortisol.

saline and administered intravenously for 30 minutes at 9 AM on day 1 in all patients to estimate the interpatient variability of CYP3A4 activity. After cortisol administration, the urine was collected for 24 hours. The total volume of the 24-hour collection was recorded, and a 5-mL aliquot was analyzed immediately.

Docetaxel Administration

Docetaxel (Taxotere; Aventis Pharm Ltd, Tokyo, Japan) was obtained commercially as a concentrated sterile solution containing 80 mg of the drug in 2 mL of polysorbate 80. In the BSA-based arm, a dose of 60 mg/m^2 of docetaxel was diluted in 250 mL of 5% glucose or 0.9% saline and administered by 1-hour intravenous infusion at 9 AM to all patients.

In the individualized arm, individualized dose of docetaxel was calculated from the estimated CL and the target AUC of 2.66 mg/L · h using the following equations:

$$\text{Estimated CL (L/h/m}^2) = 31.177 + (7.655 \times 10^{-4} \times \text{total-6-}\beta\text{-OHF [}\mu\text{g/d]}) - (4.02 \times \text{AAG [g/L]}) - (0.172 \times \text{AST [U/L]}) - (0.125 \times \text{age [years]})^{30}$$

$$\text{Individualized dose of docetaxel (mg/m}^2) = \text{estimated docetaxel CL (L/h/m}^2) \times \text{target AUC (2.66 mg/L} \cdot \text{h)}$$